

Advanced Biosystems

Microfluidic Technology for Nucleic Acid Aptamer Evolution and Application

--Manuscript Draft--

Manuscript Number:	adbi.201900012R1
Full Title:	Microfluidic Technology for Nucleic Acid Aptamer Evolution and Application
Article Type:	Invited Review
Section/Category:	
Keywords:	
Corresponding Author:	Julian Alexander Tanner, Ph.D. University of Hong Kong Pokfulam, HONG KONG
Corresponding Author Secondary Information:	
Corresponding Author's Institution:	University of Hong Kong
Corresponding Author's Secondary Institution:	
First Author:	Lewis A. Fraser
First Author Secondary Information:	
Order of Authors:	Lewis A. Fraser Yee-Wai Cheung Andrew Kinghorn Wei Guo Simon C.C. Shiu Chandra Jinata Mengping Liu Soubhagya Bhuyan Lang Nan Ho Cheung Shum Julian Alexander Tanner, Ph.D.
Order of Authors Secondary Information:	
Abstract:	The intersection of microfluidics and aptamer technologies holds particular promise for rapid progress in a plethora of applications across biomedical science and other areas. Here, we review the influence of microfluidics on the aptamer field, from traditional capillary electrophoresis approaches through to innovative modern-day approaches using micromagnetic beads and emulsion droplets. Miniaturising aptamer-based bioassays through microfluidics has the potential to transform diagnostics and embedded biosensing in coming years.
Additional Information:	
Question	Response
Please submit a plain text version of your cover letter here.	We submit the minor revision of the invited review article entitled "Microfluidic technology for nucleic acid aptamer evolution and application" for consideration by Advanced Biosystems. We have addressed all the reviewer comments. We look forward to hearing from you,

	Julian Tanner (on behalf of all authors)
Do you or any of your co-authors have a conflict of interest to declare?	No. The authors declare no conflict of interest.

DOI: 10.1002/ ((please add manuscript number))

Article type: Review

Microfluidic Technology for Nucleic Acid Aptamer Evolution and Application

Lewis A. Fraser, Yee-Wai Cheung, Andrew B. Kinghorn, Wei Guo, Simon Chi-Chin Shiu, Chandra Jinata, Mengping Liu, Soubhagya Bhuyan, Lang Nan, Ho Cheung Shum^{}, Julian A. Tanner^{*}*

Dr. L. A. Fraser, Dr. Y.W. Cheung, Dr. A.B. Kinghorn, S.C.C. Shiu., C. Jinata, M. Liu, Dr.

J.A. Tanner

School of Biomedical Sciences

LKS Faculty of Medicine

The University of Hong Kong

Hong Kong (SAR), China

Email: jatanner@hku.hk

Dr. W. Guo, L. Nan, Dr. H.C. Shum

Department of Mechanical Engineering

Faculty of Engineering

The University of Hong Kong

Hong Kong (SAR), China

Email: ashum@hku.hk

Keywords: Microfluidics, Aptamers, Selection, SELEX, Biosensors.

Abstract

The intersection of microfluidics and aptamer technologies holds particular promise for rapid progress in a plethora of applications across biomedical science and other areas. Here, we review the influence of microfluidics on the aptamer field, from traditional capillary electrophoresis approaches through to innovative modern-day approaches using micromagnetic beads and emulsion droplets. Miniaturising aptamer-based bioassays through microfluidics has the potential to transform diagnostics and embedded biosensing in coming years.

1. Introduction

This review will focus on the cross-section of two rapidly developing areas: nucleic acid aptamers, and microfluidics. The microfluidic selection of aptamers will encompass solution-phase, bead-based and droplet-based microfluidic aptamer selections. Additionally, aptamer-based microfluidic sensors will be discussed including biosensors, whole cell biosensing, protein sensing, small molecule detection and nanostructure-mediated sensing.

1.1 Aptamers

Nucleic acids are generally regarded as the polymeric molecules that store and pass genetic information across generations, and enable protein production. Across biology, it is now clear that nucleic acids play a plethora of roles in a number of processes. Across biotechnology and nanotechnology, there has been major progress in use of nucleic acids for a wide range of applications. One of these technologies has been in approaches for the *in vitro* evolution and application of nucleic acid aptamers. Aptamers are short, single-stranded nucleic acids which are capable of specific high affinity binding. Binding is facilitated by various noncovalent interactions including hydrogen bonding, van der Waals interactions, electrostatic interactions, and broadly by shape complementarity. Aptamers can bind a wide range of targets including various biological macromolecules, whole cells, surfaces or small molecules. Systematic evolution of ligands by exponential enrichment (SELEX) is the method by which aptamers are isolated, originally developed by the laboratories of Ellington, Szostak and Tuerk, Gold.^[1] SELEX is an iterative process that involves selection of nucleic acids from a massive library of random sequence oligonucleotides for a particular characteristic, typically binding. In each SELEX round the oligonucleotide library is incubated with that target molecule followed by wash steps to remove non-binding aptamers, leaving just the tightly bound aptamers that are subsequently amplified by PCR. The amplified strands from the previous round form a new

1 enriched library used in subsequent rounds of SELEX. Several rounds of SELEX enrichment
2 result in an aptamer library that tightly binds to the target of interest. These aptamers are
3
4 sequenced and characterised for affinity and specificity. Aptamers can be selected with high-
5
6 affinity K_d values in the pM to nM range.^[2] Relative to their often contrasted counterpart
7
8 protein antibodies, nucleic aptamers can be simply synthesised through solid phase synthesis
9
10 with little batch-to-batch variation, and typically have higher thermal stability.^[3]
11
12
13

14 The aptamer field has had its share of successes and challenges. One notable success was the
15
16 development of the Food and Drug Administration (FDA) approved aptameric drug known as
17
18 "Macugen" which targets the angiogenic cytokine vascular endothelial growth factor (VEGF)
19
20 associated with macular degeneration.^[4] Aptamers have had some impact on diagnostics,^[5]
21
22 such as the DNA aptamer developed against botulinum toxin.^[6] Aptamer potential has been
23
24 demonstrated in drug detection, such as the 'split' aptamer sensitive for cocaine in human blood
25
26 serum.^[7] The Jaffrey lab has developed fluorescent RNA for live-cell imaging and aptamer-
27
28 targeted antibody delivery.^[8] Additionally, aptamers have been integrated as functional
29
30 modular controllers of DNA nanostructures.^[9] Other emerging approaches include the use of
31
32 an extended genetic code, xeno-nucleic acids (XNAs) which has resulted in the first synthetic
33
34 genetic catalysts (XNAzymes) first described by the Holliger group.^[10]
35
36
37
38
39
40
41

42 Technologies for the directed evolution of nucleic acids aptamers by SELEX have shown
43
44 remarkable diversity, and microfluidics has had a significant impact in recent years. Capillary
45
46 electrophoresis was the first microfluidic technique to influence aptamer selection.^[11]
47
48 Subsequently, high throughput techniques using magnetic beads and emulsions in
49
50 microfluidics were developed.^[12] Emulsion-based techniques encapsulate the individual
51
52 oligonucleotide sequences within single droplets, known as clonal droplets.^[13] After clonal
53
54 droplet generation, emulsion PCR can be used such that droplets containing single
55
56 oligonucleotides undergo thermocycling to result in populations with droplets each containing
57
58
59
60
61
62
63
64
65

1 a clonal expansion of the single parent oligonucleotide .^[13] Droplets have substantially lower
2 rates of cross-reactivity and amplicon generation, which is ideal for the generation of
3 aptamers.^[13-14] Furthermore, new droplet based microfluidic techniques allow the selection of
4 nucleic acids based on their intrinsic catalytic activity.^[15] Aptamers generated by SELEX have
5 been functionalised in a range of microfluidic biosensors.^[16] These approaches have increased
6 the portability, automation, throughput and sensitivity of various aptamer-based assays, thus
7 enhancing aptamer-based biosensing.
8
9
10
11
12
13
14
15
16

17 **1.2 Microfluidics**

18
19 As a technology to manipulate and control liquid and particles in micro channels, microfluidics
20 has had impact across a range of fields including biology, chemistry and materials science.^[17]
21 Since the development of microfluidics in the early 1990s, numerous techniques have been
22 developed to realise multiple functions, including rapid reactions, precise liquid manipulation,
23 and inter-chip analysis of target samples.^[18]
24
25
26
27
28
29
30
31
32

33 The most basic function of microfluidics is to speed up reactions within small volumes. At the
34 micron and submicron scales of microfluidic channels, the surface-to-volume ratio is several
35 orders higher than in bulk systems, resulting in more atomic exposure during reactions.^[19] A
36 reduction in the length scale will dramatically accelerate the diffusion process with a time scale
37 of $\overline{t_d} \sim l^2/D$, where D is the diffusion coefficient of the samples. Thus, more efficient
38 chemical and biological reaction times are achieved.^[20] Active mechanical forces, such as
39 acoustic actuation and electrokinetic actuation, are often implemented into the channel to
40 accelerate mixing, further decreasing reaction times.^[21] Moreover, droplet microfluidics
41 segments the continuous flow of a bulk solution into discrete volumes in the form of droplets.
42
43
44
45
46
47
48
49
50
51
52
53
54
55
56
57
58
59
60
61
62
63
64
65

1
2
3
4
5
6
7
8
9
10
11
12
13
14
15
16
17
18
19
20
21
22
23
24
25
26
27
28
29
30
31
32
33
34
35
36
37
38
39
40
41
42
43
44
45
46
47
48
49
50
51
52
53
54
55
56
57
58
59
60
61
62
63
64
65

In addition to utilizing the natural advantages of microfluidics, passive structures and active interventions are increasingly imposed in microfluidic channels to allow manipulation of liquid samples. Passive techniques mainly comprise of trapping structures for immobilisation,^[23] and can be coupled to specific channel geometries for sample processing, such as cell separation and cell lysis.^[24] These methods are considered simple and convenient to implement, but there can be issues with robustness and efficiency due to the lack of control.^[25] In comparison, active methods, whereby external forces are applied such as dielectrophoresis (DEP), magnetic force, optical tweezers and surface acoustic waves (SAW) are more controllable, precise, and enable programmable manipulation at high temporal and spatial resolutions.^[26] Furthermore, with the advent of droplet technologies, different microfluidic modules can be combined to realise a series of droplet-based sample manipulations, from target encapsulation, polymerase chain reaction (PCR) to droplet sorting.^[27]

Advanced methods for the detection and analysis of desired targets can be performed in microfluidic channels. A series of detection techniques can be implemented into microfluidics to examine both morphologies and contents of droplets. Optical imaging is a direct observation method, aiming at monitoring morphological change of droplets under physiological conditions.^[28] Similarly, fluorescence detection can be performed to quantify the intensity of a reaction and to determine the concentration of specific molecules.^[29] More sophisticated detection methods are based on additional measurement elements. For example, the utilisation of deposited electrodes and adherent biological probes to detect current variation and concentration of specific molecules.^[30] Additionally, force sensor and on-chip probes are frequently used to measure the stiffness, deformability, and mechanical properties of target containing samples.^[31]

2 Microfluidic selection of aptamers

1 The *in vitro* selection of aptamers is achieved using SELEX, which consists of iterative rounds
2 of target incubation, partitioning and amplification.^[14] Although conventional SELEX
3 protocols are straightforward and well-established, alternative selection approaches are
4 continuously being developed. Alternative methods are required as conventional SELEX has
5 relatively poor partitioning, can be time and labour consuming, and is typically only capable
6 of selection for binding and simple single-turnover reactions. The partitioning stage is critical
7 for aptamer selection, therefore techniques with high separation efficiency which allow for
8 selection of exotic properties are of great utility.

19 **2.1 Solution phase microfluidic aptamer selection**

21 Capillary electrophoresis (CE) is a microfluidic approach developed in the early 1980's as an
22 alternative analytical technique to gel electrophoresis and liquid chromatography.^[11, 32] The
23 separation of molecules by using CE mainly relies on two mechanisms, electrophoretic
24 mobility and electroosmotic flow, within a capillary with a charged inner wall. Electrophoretic
25 mobility fractionates molecules based on their electrophoretic force, whereas electroosmotic
26 flow is driven by the difference in potential across the capillary wall and the molecules.
27 Usually electroosmotic flow is a stronger force than electrophoretic mobility, therefore net
28 migration is typically towards the cathode. CE was used for the partitioning step in SELEX, a
29 method accordingly termed CE-SELEX.^[33] Aptamers against immunoglobulin E (IgE) were
30 identified in just four rounds and showed nanomolar affinity to their selection target. As ten or
31 more rounds of conventional SELEX are required to isolate aptamers, this significant reduction
32 in selection rounds demonstrated the efficiency of applying CE to aptamer selection. An
33 alternative application of CE, so-called non-equilibrium capillary electrophoresis of
34 equilibrium mixture (NECEEM) was also demonstrated (Figure 1a).^[34] NECEEM differs from
35 CE-SELEX in that no amplification steps are used between CE partitioning rounds. NECEEM
36 is a one-round selection approach that involves several rounds of partitioning by CE and only

1 a single round of PCR amplification at the end of the selection process.^[35] Based on the success
2 of NECEEM-based aptamer selection, many more aptamers have been identified, including
3
4 aptamers against thermostable DNA mismatch binding protein (MutS),^[36] signal transduction
5
6 proteins,^[37] bovine catalase and tau protein.^[38]
7
8

9 Although NECEEM has allowed for aptamer selection using only a single PCR amplification
10
11 step after the partitioning stage, one drawback is the very low amount of template collected
12
13 from CE. This makes it difficult to obtain a high PCR yield without contamination by non-
14
15 specific amplicons. Emulsion PCR (ePCR) is a technique in which a PCR reaction mixture is
16
17 compartmentalized into a water in oil emulsion. The compartmentalization of reagent droplets
18
19 in ePCR means that deleterious non-specific amplicons are contained and cannot spread and
20
21 consume PCR products in other droplets. The addition of ePCR to NECEEM further improved
22
23 this aptamer selection technique. Krylov and colleagues have demonstrated the power of ePCR
24
25 incorporated NECEEM by selecting aptamers against an unstable protein, AlkB homologue 2,
26
27 which is a very challenging target for conventional SELEX.^[39] The significant reduction in
28
29 selection rounds demonstrated the utility of applying CE to aptamer selection.
30
31
32
33
34
35
36

37 **2.2 Bead-based microfluidic aptamer selection**

38
39 Magnetic beads have been widely implemented for the solid support immobilization of
40
41 molecular targets in SELEX since their first use in 1997.^[40] The principle behind magnetic
42
43 bead-based SELEX partitioning is very simple. In brief, targets covalently immobilized to
44
45 micro-beads are used to separate target binding DNA of interest. However, in terms of the
46
47 separation efficiency and practicality, magnetic bead based separation is inferior to other
48
49 partitioning approaches such as capillary electrophoresis.^[41] To address this issue, novel
50
51 magnetic SELEX techniques were developed that make use of microfluidic systems.^[12]
52
53
54
55

56 The Soh group pioneered the integration of magnetic bead-based SELEX with microfluidic
57
58 systems. They developed a continuous-flow magnetic activated chip-based separation
59
60
61
62
63
64
65

1 (CMACS) device (Figure 1b).^[12] In this chip, the aptamer library is bound to the target
2 immobilized beads which are guided by a magnetic field to travel along a nickel surface to a
3 product outlet. The unbound aptamers were collected through waste outlets. In just a single
4 round of selection using this device, an aptamer pool with a K_d value of 33 nM against the light
5 chain of recombinant *Botulinum* neurotoxin type A was isolated. Though the results were
6 promising, the CMACS device was limited in some respects by delicate manual performance
7 and flow stream disruptions caused by microbubbles or blockages.^[12]
8
9

10 To address these issues, Soh *et al.*, 2009 developed another microfluidic device called a Micro-
11 Magnetic Separation (MMS) chip.^[42] Compared to the CMACS device, this MMP chip was
12 fabricated with grids of ferromagnetic materials (titanium and nickel) producing magnetic field
13 gradients that can be magnetized externally. With this device, aptamers that targeted the
14 streptavidin-conjugated magnetic beads were first captured in the channel by application of an
15 external magnetic field, whilst unbound aptamers were removed by a continuous washing
16 buffer stream. Afterwards, the adhered nucleic acids could be released and collected through
17 the outlet by removing the magnet field. Aptamers against streptavidin were obtained within
18 three positive rounds of selection, and their specificities were further enhanced through another
19 round of negative selection. So far, this MMS chip had exhibited comparable or better recovery
20 (~99.5 %) and partition efficiency (10^6) when compared to those achieved in the CMACS
21 chip.^[12] Additionally, this method was faster as it allowed higher flow rates (>10 mL/h).
22 Furthermore, it was the first study that integrated both positive and negative selections in one
23 microfluidic device. Based on this chip, Soh *et al.*, 2010 selected aptamers against PDGF-BB
24 and streptavidin through introducing some optimizations such as highly stringent selection
25 conditions,^[43] which resulted in aptamers with higher affinity and specificity. Similarly, Wang
26 *et al.*, 2014 developed optimized magnetic beads-assisted microfluidic systems for screening
27 aptamers against myoglobin, which integrated both positive and negative selections.^[44] While
28
29
30
31
32
33
34
35
36
37
38
39
40
41
42
43
44
45
46
47
48
49
50
51
52
53
54
55
56
57
58
59
60
61
62
63
64
65

1 the Soh group performed the two types of selections individually,^[12] Wang *et al.*'s chip was
2 able to perform a positive selection directly after negative selection. After seven rounds of
3 selection, aptamers against myoglobin with bulk K_d value ranging from 4.93 to 6.38 nM were
4 successfully screened.
5
6

7
8
9 The above-mentioned bead-based microfluidic selection methods have focused on the
10 partitioning step. SELEX consists of many other steps including target-aptamer library
11 incubation, PCR amplification, and affinity/specificity evaluations. Microfluidic systems have
12 potential for highly integrated SELEX in a single chip so the next stage was to develop novel
13 microbead-based microfluidic SELEX platforms integrated with multiple functional units.
14
15
16

17 The first fully SELEX integrated microfluidic system was developed by the Gwo-Bin Lee
18 group. Inspired by the automatic microfluidic SELEX system proposed by Hybarger *et al.* and
19 the bead-based microfluidic system developed by Soh *et al.*^[12, 45], They fabricated a
20 microfluidic system comprising of three functional units; a microfluidic control unit, a bead-
21 based aptamer extraction unit and a PCR unit.^[46] This platform performed target-aptamer
22 incubation, aptamer separation and on-chip PCR amplification in parallel. An aptamer was
23 successfully screened against C-reactive protein (CRP) with K_d value as low as 3.51 nM in a
24 rapid manner (60 min/round). Lee *et al.* further optimized their integrated magnetic chip by
25 coupling it with a competitive assay chip, which improved the selection as it enabled immediate
26 affinity and specificity measurements of the aptamer pool directly after extraction.^[47] The
27 entire SELEX process took only 20 min which represents a dramatic reduction to time and cost
28 of an aptamer selection. Using a similar technique, Lin *et al.* screened two specific aptamers in
29 just 70 min against hemoglobin A1c and hemoglobin with K_d values at 7.6 nM and 7.3 nM
30 respectively.^[48] Subsequently, an integrated microfluidic system was developed by Kim *et al.*
31 that coupled the affinity selection and amplification step by an electrophoretic oligonucleotide
32 manipulation scheme. This allowed for the rapid selection of aptamers against either surface-
33
34
35
36
37
38
39
40
41
42
43
44
45
46
47
48
49
50
51
52
53
54
55
56
57
58
59
60
61
62
63
64
65

1 immobilized protein (immunoglobulin E) or solution-phase small molecule (bisboronic acid-
2 glucose mixture) with high affinity.^[49]
3

4 Bead-based microfluidic aptamer selection makes SELEX more rapid, efficient and ultimately
5 lowers the costs. One drawback of the previously mentioned bead-based microfluidic aptamer
6 selection systems is that the aptamer extraction step cannot be monitored on chip, therefore
7 selection round failure would not be detected until all SELEX rounds are complete. To
8 overcome this problem, Hong *et al.*, 2017 combined the selection chip with a fluorescent signal
9 evaluation system, which monitors target-coated magnetic nanospheres.^[50] The ssDNA
10 aptamer pools were FAM-labelled such that when they were incubated with targets in the
11 evaluation chip for 2 hours at a low flow rate, the fluorescent intensity of bound DNA could
12 be measured to monitor bulk binding affinity *in situ.* , Hong *et al.*, 2019 improved upon this
13 microfluidic selection setup by efficiency via trapping magnetic nanospheres on microscale.^[51]
14 It took just three selection rounds to select nanomolar dissociation constant aptamers against
15 Ebola antigens.^[51]
16
17
18
19
20
21
22
23
24
25
26
27
28
29
30
31
32

33
34 Another potential drawback with magnetic bead immobilization is the nonspecific interactions
35 of oligonucleotides to the bead surface. Carboxylic acid-coated beads that are negatively
36 charged, and hence electrostatically repel DNA, have been useful in addressing the nonspecific
37 binding problem.^[12] Despite these drawbacks, bead-based microfluidic aptamer selection
38 greatly enhances partitioning and streamlines the selection process when compared to
39 conventional SELEX.
40
41
42
43
44
45
46
47
48
49

50 **2.3 Droplet based microfluidic aptamer selection**

51
52 *In vitro* compartmentalization (IVC) is a powerful tool, creating clonal droplets and facilitating
53 high throughput single molecule species analysis. This technology is especially useful in
54 directed molecular evolution. IVC has applications in the directed molecular evolution of
55 enzymes and functional nucleic acids.^[15, 52] In this section we will focus on IVC impact on the
56
57
58
59
60
61
62
63
64
65

1 directed evolution of functional nucleic acids in the form of aptamers and ribozymes. Generally
2 nucleic acid aptamers have been selected for binding. However, more complex characteristics
3 have been selected such as fluorogenicity and catalysis including nuclease and Diels-Alder
4 cycloaddition activity.^[15, 52c, 53] IVC directed evolution is particularly suited to selection for
5 these activities as the compartmentalization links a genotype with a phenotype, consisting of
6 sequence information and activity respectively.
7

8
9
10
11
12
13
14 RNA aptamers against fluorogenic compounds are useful for RNA imaging in cells as well as
15 sensing and diagnostics. Paige *et al.*, 2011 used binding capture selection to isolate RNA
16 aptamers against the fluorogenic compound DFHBI.^[53] When DFHBI is in its native state no
17 fluorescence is observed, however when its aptamer is bound the complex exhibits a strong
18 fluorescent signal. The brightest aptamer isolated against DFHBI was termed “Spinach” due
19 to the green fluorescent signal produced. The spinach aptamer was used for RNA tracking in
20 cells,^[53] detection of metabolites and as a split aptamer.^[54]
21
22
23
24
25
26
27
28
29
30

31 Using the Spinach aptamer sequence as a starting point, Autour *et al.*, 2016 performed
32 microfluidic directed evolution to improve the spinach aptamer’s performance.^[13] A total of
33 five rounds of microfluidic selection were performed: two enrichment rounds followed by one
34 mutation round and then two enrichment rounds. A selection round consisted of emulsification
35 of PCR reaction mix containing the aptamer library in a Poisson distribution, thermal cycling
36 of PCR droplets, fusion of PCR droplets with *in vitro* transcription droplets containing DFHBI
37 fluorogen, incubation and FADS (Figure 1c). Autour *et al.* selected aptamers that displayed
38 fluorescent activity in a variety of salt conditions including K⁺, Na⁺, Li⁺, Cs⁺ and no salt. ^[13]
39
40
41
42
43
44
45
46
47
48
49
50
51 The relative molar fluorescence of the DFHBI/iSpinach complex was greater than that of
52 DFHBI/Spinach2 by 1.4 times in K⁺ buffer and by 2.1 times in Na⁺ buffer. ^[13]
53
54
55

56 Dolgosheina *et al.*, 2014 used binding capture selection to isolate RNA aptamers against the
57 fluorogenic compound Thiazole Orange.^[55] This fluorescence upon binding aptamer was
58
59
60
61
62
63
64
65

1 termed “Mango”. As for the Spinach aptamer fluorophore pair, when Thiazole Orange is in its
2 native state no fluorescence is observed, however when the Mango aptamer is bound the
3 complex exhibits a strong fluorescent signal. To isolate aptamers against Thiazole Orange,
4 twelve rounds of classical SELEX were performed. Interestingly the resulting aptamers bound
5 to biotinylated Thiazole Orange but not native Thiazole Orange. ^[55] The Mango
6 aptamer/fluorogen pair was used for single molecule imaging, was expressed in bacteria, and
7 injected into *Caenorhabditis elegans* for imaging. ^[55]

8
9
10
11
12
13
14
15
16 Autour *et al.*, 2018 used the 12th round library from the work of Dolgosheina *et al.*, 2014 and
17 performed 10 rounds of FADS selection. ^[56] One limitation of FADS is that 100 nM of TO1-B
18 was required for effective fluorescent detection of the droplets. The dissociation constant of
19 the original aptamer was 3.2 ± 0.7 nM, so improving upon aptamer dissociation constant by
20 decreasing TO1-B concentration was not feasible. Instead, a competition assay was used to
21 challenge the aptamer/TO1-B interaction with N-methyl mesoporphyrin IX (NMM) and TO3-
22 B. For the 1st to 4th selection rounds, NMM from 3 μ M to 8 μ M was used and for the 2nd to 9th
23 selection rounds TO3-Biotin was used from 3.5 nM to 230 nM. ^[56] In addition to molecular
24 competition, the stability of the RNA/TO1-B complex was challenged by sorting the droplets
25 at 45 °C. The resulting aptamers exhibited fluorescence signal eight times greater than that of
26 the original Mango aptamer when measured at 37 °C. ^[56]

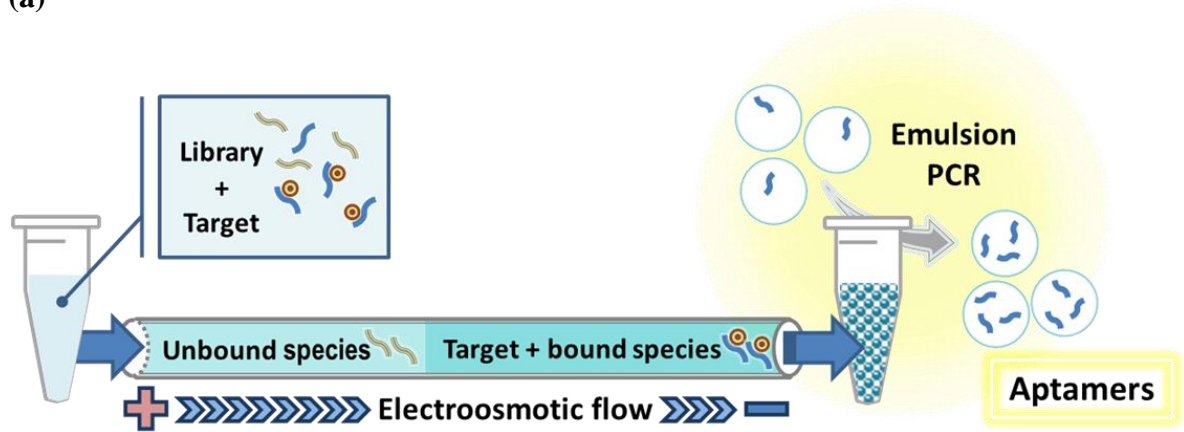
27
28
29
30
31
32
33
34
35
36
37
38
39
40
41
42
43 An important reaction in synthetic chemistry is the Diels-Alder [4 + 2] cycloaddition
44 reaction, ^[15] which occurs between a 1,3 diene and an alkene dienophile. IVC was used to select
45 for ribozymes that catalyse multiple-turnover Diels–Alder cycloadditions. ^[15] The selection
46 strategy was to covalently label an entire ribozyme gene library with anthracene, a Diels–Alder
47 cycloaddition substrate. After IVC of single DNA templates and transcription, any active
48 ribozyme would react the supplemented biotin-maleimide to the library linked anthracene,
49 thereby labelling the ribozyme encoding DNA with biotin. Since the IVC isolates each library
50
51
52
53
54
55
56
57
58
59
60
61
62
63
64
65

1 member and its respective ribozymes, there is no cross reactivity between different library
2 members and ribozymes and the connection between genotype (DNA) and phenotype
3 (ribozyme activity) is covalently linked. The emulsion is then broken and the biotinylated DNA
4 is isolated using streptavidin coated para-magnetic beads, before PCR amplification. To
5 achieve multiple-turnover selection conditions, free anthracene is emulsified with the library.
6
7 After eleven rounds of selection nearly all ribozymes contain a common catalytic motif with
8 similar activity. The best ribozyme had a turnover rate (k_{cat}) of $0.33 \pm 0.06 \text{ s}^{-1}$.^[15] Although
9 the actual partitioning step was not performed in a microfluidic device, the association of biotin
10 with DNA led to selection of higher performance ribozymes such that the selection step was
11 performed within droplets.
12

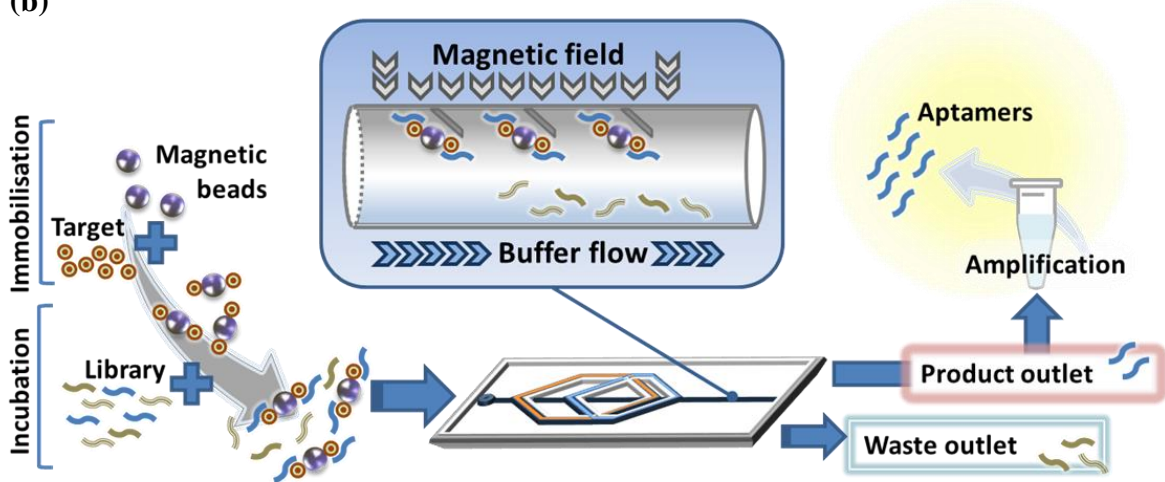
13 Using a self-cleaving RNA SELEX selection method, Tang and Breaker 2000 selected an RNA
14 cleaving ribozyme.^[52c] The dominant species isolated from the selection was the X-motif.
15 Although a relatively fast ribozyme, the X-motif's steady state turnover (k_{cat}^{SS}) was ~20-fold
16 lower than the apparent turnover during the pre-steady state burst phase (k_{burst}). This indicates
17 that the rate-limiting step of the reaction is product release. To address the rate-limiting product
18 release of X-motif, Ryckelynck *et al.*, 2015 performed a droplet-based microfluidic selection
19 to select for nuclease activity under multiple turnover conditions.^[52c] Cycles of random
20 mutagenesis and selection were performed to evolve the X-motif. The microfluidic selection
21 consisted of PCR mixture emulsification, thermocycling, fusion of *in vitro* transcription
22 mixture with PCR droplets, incubation to allow for transcription, pico-injection of activity
23 assay mixture, incubation to allow assay development and fluorescence activated sorting. After
24 nine rounds of microfluidic selection they obtained X-motif variants with a steady state
25 turnover (k_{cat}^{SS}) ~28-fold higher than the original X-motif.^[52c] This increase was primarily due
26 to an increase in the rate of product release, which was the original X-motif's rate-limiting step
27 in a multiple-turnover reaction setting.
28
29
30
31
32
33
34
35
36
37
38
39
40
41
42
43
44
45
46
47
48
49
50
51
52
53
54
55
56
57
58
59
60
61
62
63
64
65

1 IVC is a powerful tool which has been used in many research areas. Utilizing IVC for the
2 selection of nucleic acid aptamers has expanded the potential selection repertoire from simple
3 binding and single turnover catalysis to more exotic properties such as turn on fluorescence
4 upon binding and multiple turnover catalysis. A great potential exists for selection for other
5 properties, just so long as the assay can be monitored fluorometrically. IVC technologies such
6 as droplet generation, droplet merger, pico-injection and droplet sorting are under continuous
7 advancement, ^[13] and will lead to faster, higher throughput selections which will allow for
8 greater sequence space coverage and greater selection success. IVC is ideally suited to nucleic
9 acid aptamer selection.
10
11
12
13
14
15
16
17
18
19
20
21
22
23
24
25
26
27
28
29
30
31
32
33
34
35
36
37
38
39
40
41
42
43
44
45
46
47
48
49
50
51
52
53
54
55
56
57
58
59
60
61
62
63
64
65

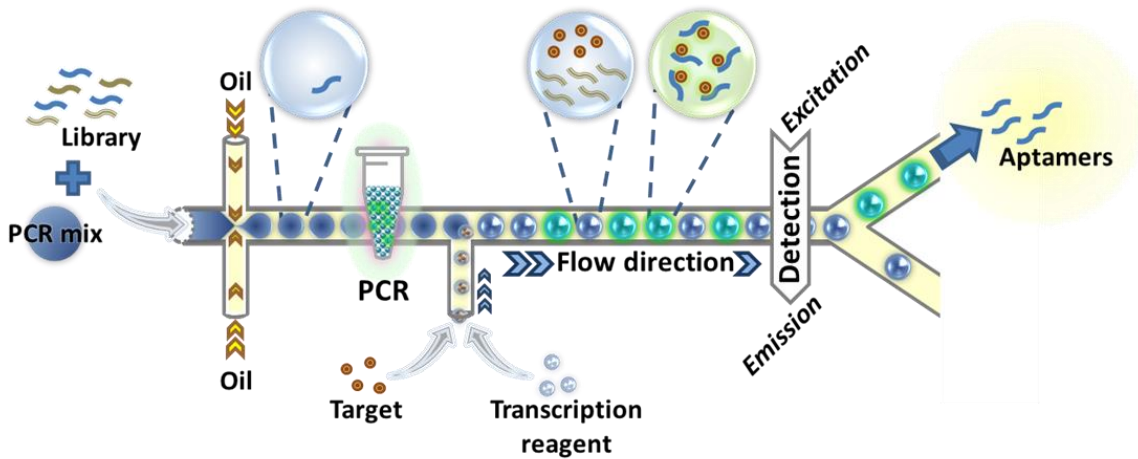
(a)



(b)



(c)



1
2
3
4
5
6
7
8
9
10
11
12
13
14
15
16
17
18
19
20
21
22
23
24
25
26
27
28
29
30
31
32
33
34
35
36
37
38
39
40
41
42
43
44
45
46
47
48
49
50
51
52
53
54
55
56
57
58
59
60
61
62
63
64
65

Figure 1. Schematic of different microfluidic aptamer selection approaches. a) Solution phase microfluidic aptamer selection. Aptamer library and target are incubated together before being injected into a capillary to undergo non-equilibrium capillary electrophoresis of equilibrium mixture (NECEEM). Target bound species are separated before emulsion PCR (ePCR) for reliable amplification of low abundance template. b) Bead-based microfluidic aptamer selection. Target immobilised to magnetic beads is incubated with the aptamer library. The mixture is then injected into the microfluidic device and the magnetic beads are held in place using an external magnetic field. Aptamers bound to the target-coated beads are guided by Ni strips and eluted through the product outlet, while unbound aptamers are diverted to the waste outlet. The binding aptamers are further transported for PCR amplification. c) Droplet based microfluidic aptamer selection. An aqueous phase made up of DNA library and PCR mix is emulsified within a microfluidic system, before PCR amplification to create monoclonal droplets. These droplets are then merged with droplets containing transcription reagent and fluorogenic target molecule before incubation at 37°C to allow transcription. Droplets then undergo FADS to select for fluorescence-activating RNA aptamers.

3.1 Aptamer based microfluidic biosensors

Aptamer-based microfluidics enable biosensors to sensitively detect a range of biomarkers. Microfluidics are ideal for biosensing as channels use lower sample volumes, which allows for more efficient use of reagents and biological samples. Microfluidic chips can be combined for multiplexed detection of multiple analytes^[16a] and flow rates, velocity, and the internal architecture of microfluidic channels can be optimised to improve binding capacity.^[16b, 16c] Furthermore, microfluidic channels can be designed to manipulate, process and separate components of complex biological samples,^[16d] for example the separation of blood components in live animal blood for detection of small molecule biomarkers.^[16e] Additionally, aptamers are perfect candidates for integration into microfluidic biosensors as they are durable

1 across a range of conditions^[3] and are smaller than antibodies, so therefore can be densely
2 packed into microfluidic channels.^[57] Here we discuss how aptamer integration with
3 microfluidics has led to highly effective biosensors for the detection of whole cells, proteins
4 and small molecules.
5
6
7
8
9

10 **3.2 Whole cell biosensing**

11 A range of aptamer-based microfluidics have been generated for the detection of whole cells.
12
13 Aptamers can be selected to bind specific proteins on the surface of cell^[58] and to proteins in
14 their native state on live cells without previous knowledge of the exact protein biomarker.^[59]
15
16 Furthermore, aptamers can be combined in cell specific ‘cocktails’ to increase specificity and
17 overcome cellular heterogeneity.^[60] The majority of microfluidic cell-based detection reports
18 have focused on the detection of circulating tumour cells (CTCs). However, aptamer-based
19 microfluidic biosensors have also been successfully developed for other cell detection
20 applications, including for the detection of bacterial cells. **Figure 2** presents a generalised
21 scheme which describes the key steps in aptamer-based microfluidic CTC capture biosensors.
22
23
24
25
26
27
28
29
30
31
32
33
34
35

36 *3.2.1 Detection of circulating tumour cells*

37
38
39
40
41
42
43
44
45
46
47
48
49
50
51
52
53
54
55
56
57
58
59
60
61
62
63
64
65
66
67
68
69
70
71
72
73
74
75
76
77
78
79
80
81
82
83
84
85
86
87
88
89
90
91
92
93
94
95
96
97
98
99
100
101
102
103
104
105
106
107
108
109
110
111
112
113
114
115
116
117
118
119
120
121
122
123
124
125
126
127
128
129
130
131
132
133
134
135
136
137
138
139
140
141
142
143
144
145
146
147
148
149
150
151
152
153
154
155
156
157
158
159
160
161
162
163
164
165
166
167
168
169
170
171
172
173
174
175
176
177
178
179
180
181
182
183
184
185
186
187
188
189
190
191
192
193
194
195
196
197
198
199
200
201
202
203
204
205
206
207
208
209
210
211
212
213
214
215
216
217
218
219
220
221
222
223
224
225
226
227
228
229
230
231
232
233
234
235
236
237
238
239
240
241
242
243
244
245
246
247
248
249
250
251
252
253
254
255
256
257
258
259
260
261
262
263
264
265
266
267
268
269
270
271
272
273
274
275
276
277
278
279
280
281
282
283
284
285
286
287
288
289
290
291
292
293
294
295
296
297
298
299
300
301
302
303
304
305
306
307
308
309
310
311
312
313
314
315
316
317
318
319
320
321
322
323
324
325
326
327
328
329
330
331
332
333
334
335
336
337
338
339
340
341
342
343
344
345
346
347
348
349
350
351
352
353
354
355
356
357
358
359
360
361
362
363
364
365
366
367
368
369
370
371
372
373
374
375
376
377
378
379
380
381
382
383
384
385
386
387
388
389
390
391
392
393
394
395
396
397
398
399
400
401
402
403
404
405
406
407
408
409
410
411
412
413
414
415
416
417
418
419
420
421
422
423
424
425
426
427
428
429
430
431
432
433
434
435
436
437
438
439
440
441
442
443
444
445
446
447
448
449
450
451
452
453
454
455
456
457
458
459
460
461
462
463
464
465
466
467
468
469
470
471
472
473
474
475
476
477
478
479
480
481
482
483
484
485
486
487
488
489
490
491
492
493
494
495
496
497
498
499
500
501
502
503
504
505
506
507
508
509
510
511
512
513
514
515
516
517
518
519
520
521
522
523
524
525
526
527
528
529
530
531
532
533
534
535
536
537
538
539
540
541
542
543
544
545
546
547
548
549
550
551
552
553
554
555
556
557
558
559
560
561
562
563
564
565
566
567
568
569
570
571
572
573
574
575
576
577
578
579
580
581
582
583
584
585
586
587
588
589
590
591
592
593
594
595
596
597
598
599
600
601
602
603
604
605
606
607
608
609
610
611
612
613
614
615
616
617
618
619
620
621
622
623
624
625
626
627
628
629
630
631
632
633
634
635
636
637
638
639
640
641
642
643
644
645
646
647
648
649
650
651
652
653
654
655
656
657
658
659
660
661
662
663
664
665
666
667
668
669
670
671
672
673
674
675
676
677
678
679
680
681
682
683
684
685
686
687
688
689
690
691
692
693
694
695
696
697
698
699
700
701
702
703
704
705
706
707
708
709
710
711
712
713
714
715
716
717
718
719
720
721
722
723
724
725
726
727
728
729
730
731
732
733
734
735
736
737
738
739
740
741
742
743
744
745
746
747
748
749
750
751
752
753
754
755
756
757
758
759
760
761
762
763
764
765
766
767
768
769
770
771
772
773
774
775
776
777
778
779
780
781
782
783
784
785
786
787
788
789
790
791
792
793
794
795
796
797
798
799
800
801
802
803
804
805
806
807
808
809
810
811
812
813
814
815
816
817
818
819
820
821
822
823
824
825
826
827
828
829
830
831
832
833
834
835
836
837
838
839
840
841
842
843
844
845
846
847
848
849
850
851
852
853
854
855
856
857
858
859
860
861
862
863
864
865
866
867
868
869
870
871
872
873
874
875
876
877
878
879
880
881
882
883
884
885
886
887
888
889
890
891
892
893
894
895
896
897
898
899
900
901
902
903
904
905
906
907
908
909
910
911
912
913
914
915
916
917
918
919
920
921
922
923
924
925
926
927
928
929
930
931
932
933
934
935
936
937
938
939
940
941
942
943
944
945
946
947
948
949
950
951
952
953
954
955
956
957
958
959
960
961
962
963
964
965
966
967
968
969
970
971
972
973
974
975
976
977
978
979
980
981
982
983
984
985
986
987
988
989
990
991
992
993
994
995
996
997
998
999
1000

CTCs are cells released into the blood stream by metastatic cancers which are capable of forming secondary metastatic tumours.^[61] Measuring CTCs can aid physicians in monitoring progression and recurrence of cancer.^[62] The first publication outlining the concept of aptamer-based CTC in a microfluidic was described by the Weihong Tan research group, in which DNA aptamers which bind to T-cell acute lymphocytic leukaemia cells with a K_d of 0.8 nM were conjugated to an avidin-coated PDMS microchannel.^[63] Solutions of dyed cells were passed through the microfluidic channel and captured cancer cells were imaged by confocal microscopy. The cancer cells were captured with a >97 % purity and a >80 % efficiency.^[63] This initial principle of aptamer capture of CTCs in microfluidic channels has been developed

1 over the last decade and aptamer based microfluidic CTC capture devices can now selectively
2 capture and release CTCs,^[64] and capture and isolate single CTC cells.^[65] A range of different
3
4 CTCs can now be captured in aptamer-based microfluidics (Table 1).
5
6

7 An advantage of using microfluidic devices is the capacity to modify internal architectures for
8 increased binding capacity and processing complex biological solutions. For example, a
9
10 microfluidic was designed which contained >59,000 aptamer coated micropillars.^[65] As a cell
11
12 containing biological samples passes through this microfluidic the micropillars increase the
13
14 probability of aptamer cell binding events by a principle known as deterministic-lateral-
15
16 displacement.^[66] This novel internal architecture allows more sample to be rapidly processed
17
18 without sample pre-treatment. As a result of the micropillars, the device captured 10 tumour
19
20 cells from 1 mL of whole blood, a >95% capture efficiency.^[65]
21
22
23
24
25
26

27 Many advances in aptamer-based microfluidics for CTC capture have focused on the analysis
28
29 of cancer cells for research purposes, such as selective capture and release of CTCs,^[67] capture
30
31 and isolation of single CTC cells,^[65] and gDNA isolation to examine genetic mutations.^[68]
32
33 However, advances have also complemented the development of biosensors for diagnostic
34
35 purposes. Fluorescent detection is typically used in CTC biosensing. CTCs are stained by
36
37 membrane staining dyes or DNA staining dyes and subsequently imaged by confocal
38
39 microscopy,^[69] a method which is less amenable to biosensor portability. However,
40
41 electrochemical detection systems are portable instrument-free detection systems. For example,
42
43 a PDMS microfluidic device was reported which uses an electrochemical method containing
44
45 EGFR binding aptamers and two integrated electrodes. Aptamer-captured CTCs are positioned
46
47 between the electrodes and specifically detected by impedance measurements.^[70] Song *et al.*,
48
49 2019 developed a lateral displacement-patterned microfluidic chip modified with multivalent
50
51 aptamer-functionalized nanospheres to improve CTC capture efficiency.^[71] They were able to
52
53 improve binding efficiency 100-fold, and multivalent capture improved capture efficiency 3-
54
55
56
57
58
59
60
61
62
63
64
65

1 fold relative to monovalent capture. The captured CTC were released using a thiol exchange
2 reaction with 80% efficiency and 96% cell viability, thus enabling compatibility with
3 downstream cellular analysis.^[71]
4
5
6

7 8 3.2.2. Detection of non-CTCs 9

10 Aptamers can be selected against a broad range of cellular motifs and applied in biosensors.
11 Consequently, they can be used to detect non-CTCs. Biosensor detection of bacterial cells is
12 of particular interest when detecting water and food-based pathogens.^[72] A biosensor was
13 developed to detect water-based *Escherichia coli*, in which a solution containing *E.coli* cells
14 was incubated with aptamer coated fluorescent nanoparticles was passed through a PDMS
15 microfluidic.^[73] The design used a sheath flow junction to focus the sample into the centre of
16 a microfluidic channel where a laser based optofluidic particle sensor counted bacterial cells
17 coated in the fluorescent nanoparticles. This method was shown to be specific against
18 alternative bacterial strains, and capable of detecting ~100 particles per second with an ~85%
19 accuracy.^[73] To our knowledge there is not currently an electrochemical aptamer based
20 microfluidic biosensor for the detection of bacterial cells, though antibody alternatives exist
21 which could benefit from innovations in aptamer research.^[74]
22
23
24
25
26
27
28
29
30
31
32
33
34
35
36
37
38
39
40
41
42
43
44
45
46
47
48
49
50
51
52
53
54
55
56
57
58
59
60
61
62
63
64
65

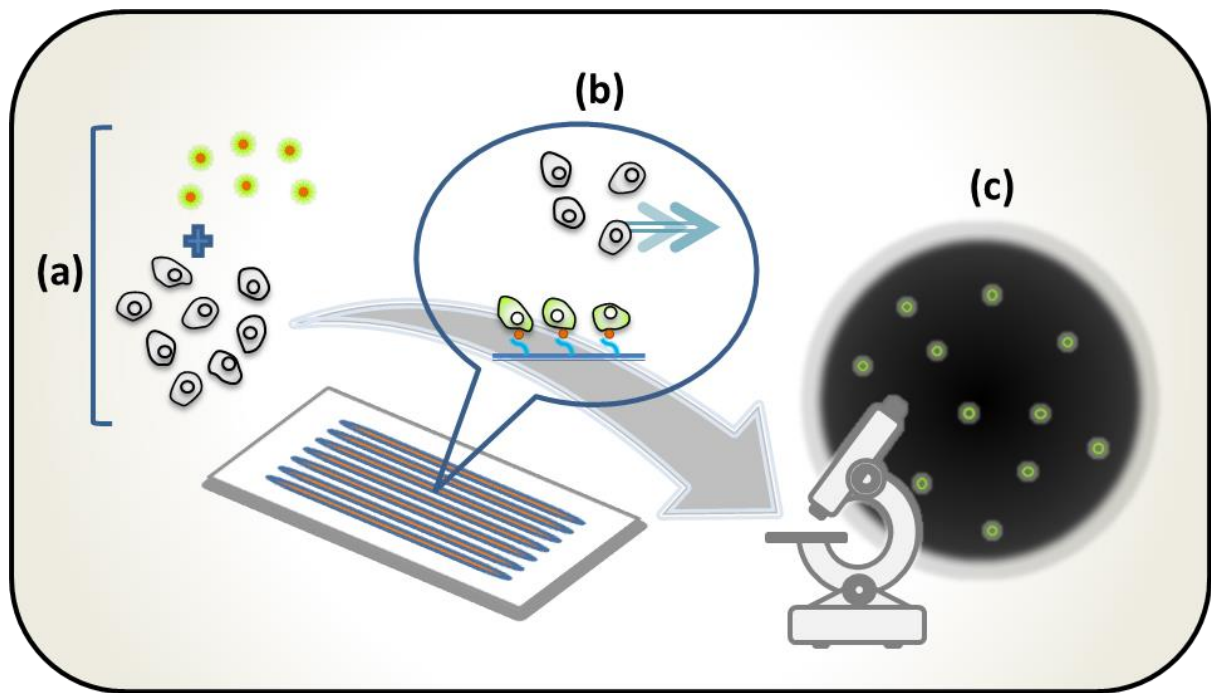


Figure 2. A generalised representation of aptamer-based CTC capture in a microfluidic. a) Cells are incubated with a cell specific fluorescent dye. b) Aptamers specifically capture CTCs whilst other cells are removed from the microfluidic in the flowing buffer. c) Cells captured in the microfluidic are observed, measured and counted by fluorescence microscopy.

3.3 Aptamer based microfluidic protein sensing

Given the advantages of aptamer based microfluidics, emerging platforms for protein sensing are being developed for diagnostics. Here we classify into three types: 1/ direct detection, 2/ sandwich assay and 3/ label-free detection.

3.3.1 Direct detection

One of the major characteristics of aptamers is the ease by which they can be chemically modified. There are well-established protocols for nucleic acid modification for labelling nucleic acids with different tags to facilitate direct detection.^[75] Figure 3A illustrates the general configuration of direct detection approach by using fluorescently labelled aptamers.

1 George Whitesides discussed the crosstalk between CE and microfluidic analytical
2 methods.^[17a] Besides aptamer selection, CE can also be applied for aptamer-based protein
3 sensing. The first aptamer based CE method for protein sensing was reported by Kennedy and
4 colleagues in 1998.^[76] They demonstrated a method by integrating two approaches of CE,
5 affinity probe capillary electrophoresis (APCE) and capillary electrophoresis with laser-
6 induced fluorescence detection (CE-LIF), for the detection of immunoglobulin E (IgE). APCE
7 is based on the separation of the target molecule bound to a fluorescence-labelled affinity probe
8 in a mixture by using CE. In Kennedy and colleagues' study, IgE was bound to a fluorophore-
9 labelled aptamer and separated by CE. The signal of the IgE-fluorophore labelled aptamer
10 complex was subsequently detected by laser induced fluorescence.^[76] Based on this approach,
11 they achieved a limit of detection (LoD) of 46 pM and detected thrombin with an LoD of 40
12 nM.
13
14
15
16
17
18
19
20
21
22
23
24
25
26
27
28

29 Recent advances in electrochemical sensing also benefit direct detection of proteins in
30 microfluidics. Liu *et al.* described a microdevice that consists of microfluidic channels and
31 aptamer-modified electrodes for detecting cytokines, interferon (INF)- γ and tumour necrosis
32 factor (TNF)- α , released from leukocytes.^[77] Thiolated aptamers were functionalised by using
33 the redox reporter methylene blue and immobilised to gold electrodes. Binding to the cytokines
34 induced a conformational change in the aptamers, shifting the redox active methylene blue
35 group resulting in a signal-off reading by square wave voltammetry due to a decrease in current.
36
37
38
39
40
41
42
43
44
45
46
47

48 3.3.2 Sandwich assay

49
50 The high specificity of aptamers not only enables them to act as signal reporters in microfluidic
51 systems, it also facilitates the specific targeting of proteins for further detection in sandwich
52 assays (Figure 3B). A method to detect interleukin-8 (IL-8) that incorporates rolling circle
53 amplification (RCA) was developed by Zhang and colleagues.^[78] Using a dual function bio-
54
55
56
57
58
59
60
61
62
63
64
65

1 chip, endothelial cells were grown in a cell culture chamber connected to a detection chamber
2 by micro-channels. The detection chamber was coated with anti-IL-8 antibodies for capturing
3 the secreted IL-8. The presence of IL-8 then was detected by using a biotinylated aptamer
4 which bound to avidin. The presence of avidin enables the binding of biotinylated RCA primers
5 for further signal amplification by RCA. The LoD of this RCA incorporated sandwich assay
6 for detection of IL-8 was 7.5 pg/mL.
7
8
9
10
11
12
13

14 Instead of coating aptamers on the surface of microfluidic channels, aptamers can also be
15 immobilised to microbeads for capturing target proteins. Conventional approaches for
16 detecting the cardiovascular disease biomarker, C-reactive protein (CRP), take 150 minutes
17 and the detection limit is 0.125mg/L.^[79] Yang and colleagues developed an automatic
18 microfluidic process for measuring C-reactive protein (CRP) by a magnetic bead-incorporated
19 microfluidic system, which significantly improved the efficiency and LoD.^[79] The advantage
20 of utilising magnetic beads in microfluidic system is related to their facile and fast separation
21 by magnetic field. Thus, targets captured on the surface of aptamer immobilised magnetic
22 beads can be efficiently isolated. In the Yang *et al.* system, aptamers were immobilised on
23 magnetic beads for capturing CRP, and the whole process is driven by micropumps,
24 microvalves and micromixers for washing and separation of unbound species. After washing
25 steps, the captured CRP was detected by antibodies for further chemiluminescence
26 measurements. With this automatic microfluidic system, lower quantities of sample and
27 reagents were required, process time was significantly reduced to 25 minutes, and the detection
28 limit was greatly improved to 0.0125mg/L.
29
30
31
32
33
34
35
36
37
38
39
40
41
42
43
44
45
46
47
48
49
50
51

52 3.3.3 Label-free detection

53 Label-free detection is another aspect of aptamer-based microfluidic detection (Figure 3C). A
54 *Plasmodium falciparum* lactate dehydrogenase (PfLDH) specific aptamer was identified by
55
56
57
58
59
60
61
62
63
64
65

1 our team (Tanner research group) ^[80] and an aptamer-tethered enzyme capture (APTEC) assay
2 which bases detection on the intrinsic enzyme activity of the captured PfLDH malaria
3 biomarker protein was developed ^[81]. It has since been incorporated to a range different
4 detection formats. ^[9d, 9e, 82] The APTEC assay was incorporated into a portable microfluidic 3D
5 printed device as a prototype point-of-care diagnostic device ^[82a]. The PflDH-specific aptamer
6 was immobilised on the surface of magnetic beads. The aptamer beads within the microfluidic
7 were incubated in patient blood samples, separated from the blood, washed, and brought into
8 the development chamber. If bound blood-borne PflDH was present on the beads, then the
9 intrinsic enzyme activity of PflDH in the development chamber resulted in the generation of
10 a colored diformazan dye which was detected by a mobile detection system. The performance
11 of this 3-D printed microfluidic device was examined by using both cultured parasites samples
12 and clinical samples and found it able to differentiate *P. falciparum* infected and uninfected
13 samples with lower detection limit of 0.01 % parasitaemia. ^[82a]

14 Colorimetric detection has also been developed for aptamer-based microfluidic protein
15 biosensing. The advantage of using colorimetric detection is that the signal can be observed by
16 the naked eye without specialised instrumentation, which favours protein sensing in closed
17 systems. A G-quadruplex DNAzyme which consists of a G-rich nucleic acid sequences that
18 forms non-canonical hemin associating structures of stacked G-tetrads shows peroxidase-
19 mimicking activity. ^[83] These DNAzyme structures are able to react with peroxidase substrates
20 to produce colorimetric signals. By incorporating G-quadruplex DNAzyme sequences with
21 aptamers, the presence of aptamer captured target can be detected. An aptamer-based
22 microfluidic system with dual chambers was developed for studying cell-to-cell
23 communication between tumour cells and endothelial cells. ^[83] To demonstrate cell-cell
24 interaction, the online analysis of cell secretory protein, vascular endothelial growth factor
25 (VEGF), was detected by DNAzyme functionalised aptamer that was coated on a microfluidic

1 channel. ^[83] On target capture the VEGF aptamer capture induced formation of the peroxidase
2 DNAzyme. ^[83] By adding hemin and chromogenic peroxidase substrate, 2,2'-azino-bis(3-
3 ethylbenzothiazoline-6-sulphonic acid) (ABTS), the aptamer captured VEGF was
4 colorimetrically observed.
5
6
7
8
9

10 Electrochemical sensing has also been applied to protein biosensing in the form of label free
11 detection. Electrochemical impedance spectroscopy (EIS) has been employed for the
12 measurements of molecular interactions. ^[84] EIS measurement is mainly based on the electron
13 transfer kinetics between a redox probe and an electrode. ^[84] The presence of target can be
14 detected by comparing the circuit resistance between the working electrode and reference
15 electrode. The EIS approach provides high sensitivity with relative simplicity, thus it is widely
16 used in biosensing. Electrochemical approaches for thrombin detection have been
17 developed,^[84] and recently it was incorporated to polydimethylsiloxane (PDMS) channel layer
18 to form microfluidic detection.^[85] In the microfluidic electrochemical thrombin aptasensor,
19 thrombin binding aptamer was immobilised on a gold working electrode and the presence of
20 thrombin was detected by measuring change in impedance once the binding event occurs. This
21 thrombin microfluidic aptasensor had a detection range of 0.1-100,000 ng/mL and a limit of
22 detection of 0.1 ng/mL. Moreover, compared with traditional electrochemical sensors, this
23 microfluidic aptasensor used less reagent and is thus more cost-efficient.
24
25
26
27
28
29
30
31
32
33
34
35
36
37
38
39
40
41
42
43
44

45 Microfluidic aptamer-based electrochemical biosensing system has also been demonstrated for
46 the cardiac damage biomarker, creatine kinase (CK)-MB. ^[86] Only trace amount of CK-MB is
47 secreted when there is cardiac damage. The current gold standard detection method is based on
48 an enzyme-linked immunosorbent assay (ELISA) that requires a substantial sample volume
49 and has low sensitivity. ^[86] By exploiting the advantages of microfluidics, Shin and colleagues
50 developed an aptamer-based electrochemical biosensor integrated with a microfluidic platform
51
52
53
54
55
56
57
58
59
60
61
62
63
64
65

for in-line detection of secreted CK-MB.^[86] This provided a sensitive, low sample approach for the detection of CK-MB.

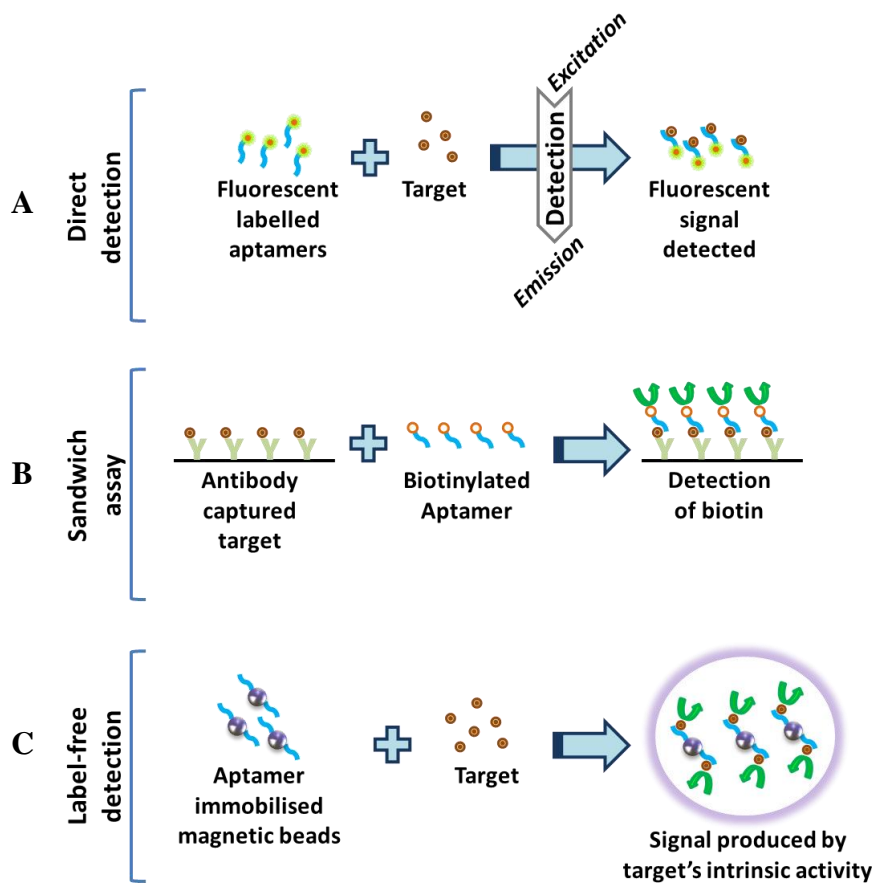


Figure 3. Schematic illustration of different aptamer based detection approaches. A) Aptamer is labelled with reporter for direct detection. B) A sandwich is formed by an antibody for capturing the target, target molecule and a biotin labelled aptamer for further visualisation. C) An example for label-free detection. The magnetic beads act as the solid support for the aptamer for capturing protein targets in sample solution. Colorimetric signal produced by the intrinsic enzyme activity of the target indicating the presence of target.

3.4 Aptamer based microfluidic small molecule detection

Adenosine and ATP are among the most thoroughly researched small molecules in microfluidic biosensor development due to their relevance in various biological reactions and their associations with disease.^[87] Commonly used detection approaches include fluorescence,

1 colorimetry, and electrochemistry. All these approaches have been applied successfully in
2 independent microfluidic systems.^[88] Zhang *et al.* applied multienzyme-linked nanoparticle
3 amplification and quantum dots labelling to achieve remarkable 0.1 pM LoD of adenosine
4 using a fluorescence based method.^[88a] In terms of colorimetric detection, many groups have
5 developed paper-based microfluidic systems (μ PADs) to realize the Point-of-Care Testing
6 (POCT) of adenosine. Tian and colleagues introduced hydrogel- μ PADs that reached 15.7 μ M
7 detection limit,^[88b] while Zhang Group created strip-like μ PADs allowing LoD of 0.16 μ M.^[88c]
8 Another facile method known as Rubik's Cube Stamping (RCS) was also utilized to fabricate
9 a rosin-patterned eight-channel μ PAD facilitating adenosine detection as low as 5.7 μ M.^[88d]
10 Additionally, chemiluminescence based alternative enabled detection of 6 μ M of adenosine
11 from 2 μ L sample.^[89] In contrast to adenosine, ATP detection generally relies on
12 electrochemical methods. Du *et al.* coupled an electrochemical probe named RuHex used
13 signal amplifying AuNPs to obtain 0.3 nM LoD for ATP.^[88e] Methods such as
14 electroluminescence (ECL) and photoelectrochemistry (PEC) were have also been explored.
15 The Huang group generated a novel porous Au-paper working electrode that embedded a
16 microfluidic origami ECL device (μ -OECLD) which allowed impressive ATP detection as low
17 as 0.1 pM.^[90] The same group further demonstrated the feasibility of their PEC origami device
18 (μ -PECOD) and achieved a 0.2 pM LoD.^[91]

19 Moreover, cocaine, various food contaminant toxin targets such as aflatoxin,^[93] botulinum
20 toxin,^[94] and ochratoxin A have all gained the attention from aptamer based microfluidic
21 researchers.^[95] The Pavesi Group developed a microring resonator to detect aflatoxin in the
22 nanomolar range.^[93b] Surface enhanced Raman spectrometry (SERS) was also introduced in a
23 microfluidic system for the detection of ochratoxin A and polychlorinated biphenyls.^[96] Due
24 to surface-enhanced effects from patterned metallic nanostructures in microfluidics, the Raman
25 signals of aptameric monolayer assemblies can be improved by several orders of magnitude

(typically 10^6 – 10^8 enhancement) as compared with standard Raman measurements.^[95c, 96]

1
2 Additionally, Kim *et al.* established a static light scattering detection method in a Y- channel
3
4 PDMS microfluidic device against oxytetracycline antibiotic, achieving a striking detection
5
6 limit of 100 ppb with a detection time of less than three minutes.^[97] Other small molecules,
7
8 such as beta-hydroxybutyrate,^[98] catecholamine,^[99] cortisol,^[100] sulforhodamine B,^[101] and
9
10 various types of antibiotics were also used as detection targets in microfluidic systems.^[102]
11
12

13
14 Microfluidic Electrochemical Detector for *In vivo* Continuous monitoring (MEDIC) was
15
16 introduced by Soh and Plaxco Groups to observe the concentration dynamics of small
17
18 molecules, particularly doxorubicin (a chemotherapeutic drug) and kanamycin (an
19
20 antibiotic)^[16e]. They were able to track the chemicals in live rats over multiple hours in real-
21
22 time and envisioned that this system could be applied to human patients.^[16e] They further
23
24 improved the system by utilizing generalizable closed-loop approach to both monitor
25
26 doxorubicin continuously and adjust the concentration of the drug in live rabbits.^[103] Other
27
28 than small molecules, detection of some metal ions through microfluidic systems has also been
29
30 explored.^[104] Mercury ions could be detected down to 5 ppb through a fluorescent lateral flow
31
32 aptamer assay in an integrated smartphone-based portable device for point-of-care
33
34 detection.^[95b] DNA aptamers for metal sensing have been suggested to be more widely
35
36 integrated in microfluidic biosensors.^[105]
37
38
39
40
41
42
43
44
45
46
47
48
49
50
51
52
53
54
55
56
57
58
59
60
61
62
63
64
65

Table 1. Examples of aptamer-based microfluidics as biosensing tools.

Category	Target	Efficiency #	Detection Method
Whole Cell	T-cell acute lymphocytic leukaemia cell line	>80% Efficiency ^[69a, 106]	Fluorescent ^[69a, 106]
	B-cell, human Burkitt's lymphoma	61% Efficiency	Fluorescent ^[69a]
	non-Hodgkin's B-cell lymphoma	50% Efficiency	Fluorescent ^[69a]
	Lymph Node Carcinoma of the Prostate Cells	90% Recovery	Electrochemical ^[67]
	Colorectal adenocarcinoma	97% Efficiency	Fluorescent ^[65]
	Dukes' type C Colorectal carcinoma	91% Efficiency	Fluorescent ^[65]
	Non-small-cell lung cancer	>95% Efficiency	Fluorescent ^[107]
	Adenocarcinoma cells	>75% Efficiency	Fluorescent ^[60]
	H460 large cell carcinoma	>50% Efficiency	Fluorescent ^[60]
	Pulmonary mucoepidermoid carcinoma cells	>50% Efficiency	Fluorescent ^[60]
	H1299 large cell carcinoma	>50% Efficiency	Fluorescent ^[60]
	Squamous carcinoma cells	>50% Efficiency	Fluorescent ^[60]
	Michigan Cancer Foundation-7 cells	94% Efficiency ^[108]	Fluorescent ^[108]
Proteins	Immunoglobulin E	LoD: 46 pM	Fluorescent ^[76]
	Thrombin	LoD: 40 nM	Fluorescent ^[76]
		LoD: 0.1 ng/mL	Electrochemical ^[85]
	Interferon interferon (INF)- γ	LoD: 60 pM	Electrochemical ^[77b]
	Tumour necrosis factor (TNF)- α	LoD: 0.58 nM	Electrochemical ^[77a]
	Interleukin-8 (IL-8)	LoD: 7.5 pg/mL	Fluorescent ^[78]
	C-reactive protein (CRP)	LoD: 0.0125mg/L	Chemiluminescent ^[79]
	<i>P. falciparum</i> lactate dehydrogenase (PfLDH)	LDL: 0.01% parasitaemia	Colorimetric ^[82a]
	Vascular endothelial growth factor (VEGF)	LoD: 1.30 ng/mL	Colorimetric ^[83]
	Creatine Kinase-MB (CK-MB)	LoD: 2.4pg/mL	Electrochemical ^[86]
Small Molecules	Adenosine	LoD: 0.1 pM	Fluorescent ^[88a]
		LDL: 15.7 μ M ^[109] , 100 μ M ^[88b] , LoD: 0.16 μ M ^[88c] , 5.7 μ M ^[88d]	Colorimetric ^[88b-d]
		LDL: 6 μ M	Chemiluminescent ^[89]
	Aflatoxin B1	LoD: 1.77 nM	Colorimetric ^[93a]
	Aflatoxin	LoD: 1.6×10^{-6} RIU	Ring resonance ^[93b]
	Ampicillin	LDL: 100 pM	Electrochemical ^[102a]
	ATP	LoD: 0.3 nM	Electrochemical ^[88e]
		LDL: 0.1 pM	Electroluminescent ^[91]
		LoD: 0.2 pM	Photoelectrochemical ^[91]
	Beta-hydroxybutyrate	LoD: 0.3 mM	Electrochemical ^[98]
	Botulinum toxin	LDL: 1 pg/ μ L	Electrochemical ^[94]
	Catecholamine	LDL: 50 μ M	Electrochemical ^[99]
	Cocaine	LoD: 4.5 μ M ^[109] , 3.8 μ M ^[88b] , 2.36 μ g ^[92a]	Colorimetric ^[88b, 92a]
		LoD: 0.5 pM ^[88a] , 10 pM ^[92b] , 0.2 μ M ^[92c]	Fluorescent ^[88a, 92b, 92c]
		LoD: 70 nM ^[88e] , LDL: 10 μ M ^[92d]	Electrochemical ^[88e, 92d]
	Cortisol	LDL: 30 pg/ mL	Electrochemical ^[100]
	Doxorubicin	LoD: 10 nM in buffer ^[16e] , 60 nM in blood ^[103]	Electrochemical ^[16e, 103]
	Kanamycin	LDL: 4.5 mM ^[16e] , 10 nM ^[102a]	Electrochemical ^[16e, 102a]
		LoD: 0.29 pg/ mL	Fluorescent ^[102b]
	Ochratoxin A	LDL: 1.27 nM	Colorimetric ^[95a]
	LoD: 3 ng/ mL	Fluorescent ^[95b]	
	LDL: 2.5 μ M	SERS ^[95c]	
Oxytetracycline	LDL: 100 ppb	Static Light Scattering ^[97]	

1
2
3
4
5
6
7
8
9
10
11
12
13
14
15
16
17
18
19
20
21
22
23
24
25
26
27
28
29
30
31
32
33
34
35
36
37
38
39
40
41
42
43
44
45
46
47
48
49
50
51
52
53
54
55
56
57
58
59
60
61
62
63
64
65

Polychlorinated biphenyls	LoD: 10 nM	SERS ^[96]
Sulforhodamine B	LDL: 0.07 μM	Fluorescent ^[101]
Tetracycline	LDL: 1 μM	Fluorescent ^[102c]

#LoD – Limit of detection; LDL – Lower detection limit

3.5 Nanostructures in Microfluidic Sensing.

1
2 Given the nature of aptamers as nucleic acids, they can be easily integrated into nucleic acid-
3
4 based nanostructures for applications in diagnostics, therapeutics and even bioelectronics. The
5
6 field of DNA nanotechnology originated from Nadrian Seeman's work on using the concept of
7
8 Holliday junctions to fabricate different two and three-dimensional lattices. ^[110] Since then,
9
10 more complicated objects have been created in the form of DNA origami. DNA origami
11
12 consists of single-stranded plasmid such as M13 used as a scaffold strand, bent into any shapes
13
14 using sequence specific staple strands.^[111] The biocompatibility of DNA has spurred research
15
16 into nanostructures for medical applications. In terms of diagnostics, simple DNA
17
18 nanostructures have been developed to detect nucleic acids target through strand displacement.
19
20 The presence of target induces the changes in distance between the parts of nanostructure,
21
22 which leads to the generation of signal.^[112] For detecting molecules other than nucleic acids,
23
24 the target recognition site of nanostructure can be replaced with target specific aptamers.
25
26 Depending on the design of structural changing mechanism, a split aptamer could be essential
27
28 in bringing parts of the structure into proximity for signal generation.^[9e]
29
30 The programmability of nucleic acids allows for the integration of different DNA
31
32 nanostructures to improve the performance of aptamer-based microfluidic systems. The Soh
33
34 group previously published the work on using microfluidics system to analyze and select the
35
36 shape-changing DNA nanostructure for cargo release upon target recognition.^[113] The typical
37
38 systematic evolution of ligands by exponential enrichment (SELEX) selects single stranded
39
40 nucleic acids for specific target binding.^[1b] Instead of doing it in the traditional way, they use
41
42 the same concept to directly select a split aptamer that could eliminate the issue of reduction in
43
44 affinity when modifying a single-stranded aptamer into a split. The two random regions of split
45
46 aptamer were incorporated to the ends of a GC-rich duplex so that the guanine rich sequence
47
48 was able to form a G-quadruplex and the duplex was intercalated with a fluorescent molecule
49
50 as a cargo. The strong binding between split aptamer and target molecule would displace the
51
52
53
54
55
56
57
58
59
60
61
62
63
64
65

1
2
3
4
5
6
7
8
9
10
11
12
13
14
15
16
17
18
19
20
21
22
23
24
25
26
27
28
29
30
31
32
33
34
35
36
37
38
39
40
41
42
43
44
45
46
47
48
49
50
51
52
53
54
55
56
57
58
59
60
61
62
63
64
65

complementary strand in the duplex leading to the formation of G-quadruplex and release the fluorescent molecule with enhanced fluorescence intensity.^[113] By using micromagnetic separation, they could isolate the complementary strand that was conjugated to streptavidin bead and measure the fluorescence signal on individual beads in the microfluidic chip.

The attachment of aptamers to the vertex of DNA tetrahedron nanostructures has been found to enhance the binding affinity of aptamers towards target molecules. The Pei group attempted to coat three different DNA tetrahedron to the inner surface of a microfluidic channel capturing three different analytes including ATP, thrombin and cocaine as shown in Figure 4A.^[114] Multiplex detection was achieved in blood serum and the biomarkers were detected within the clinical range. In addition to the reduction in cost of analysis due to the use of nanoliter droplets, detection of biomarkers in serum indicates a synergy between DNA nanostructures and microfluidics for disease diagnosis.^[114] Apart from enhancing sensitivity of detection, the sophisticated design of microfluidics chip also allows development of molecular computing approaches. Most designs of structural switching DNA nanostructures use a “burnt-bridge” mechanism, an irreversible step.^[115] With multiple inputs and computer-controlled flow rate, researchers created 64 commands to control a bipedal DNA walker to move bi-directionally on a DNA origami track with defined speed (Figure 4B – E).^[116] It was achieved by introducing fuel and antifuel strands separately in order to perform multiple strand-displacement, an example of an advanced nanostructure techniques that could have applications in aptamer based biosensing.

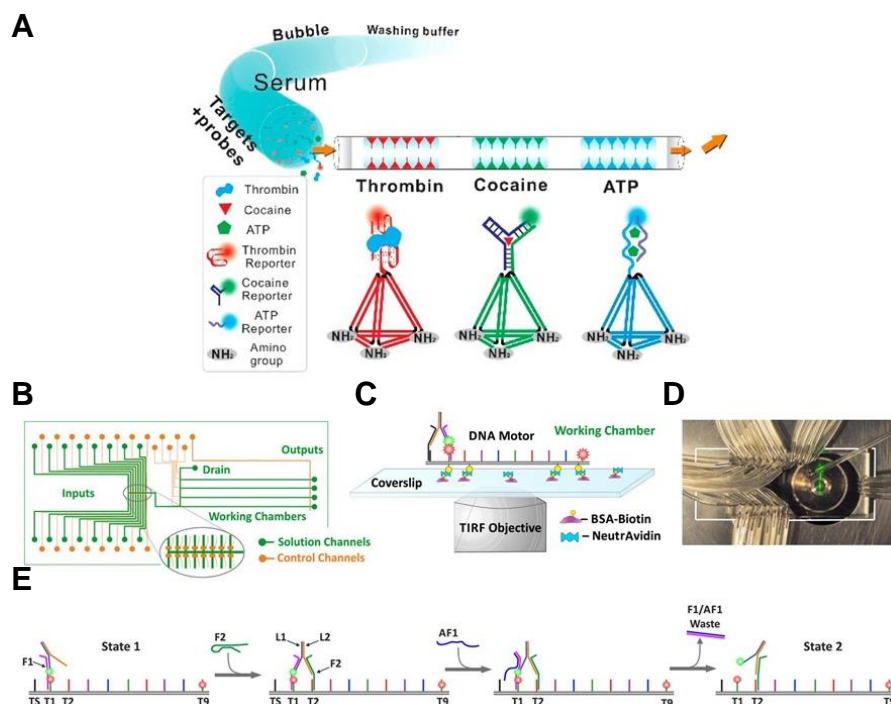


Figure 4. Integration of DNA nanostructure to microfluidics systems. A) Design of multiplex sensing using DNA tetrahedra with aptamers in microfluidic channels. Tetrahedra with amino groups extend from the bottom were coated on the inner surface of glass capillary through amine-aldehyde reaction. Different aptamers extended from the top of tetrahedra allowed simultaneous detection of thrombin, cocaine and ATP in a nanoliter droplet. B) Microfluidic device with sixteen input channels (green) with pneumatic valves (orange). The combinations allowed 64 consecutive commands of DNA strands, leading to 32 steps of a bipedal walker on a DNA origami track inside the microfluidics. C) The DNA origami walker system was immobilized on the coverslip through biotin-NeutrAvidin interaction. D) Image of the microfluidic device mounted on the TIRF setup. E) Mechanism of the walker system on DNA origami. Fuel strands (F) targeted to specific legs of walker and foothold (T) on origami would lead to precise immobilization. Antifuel strands (AF) were used to displace the fuel strands for leg detachment as completing one movement. The increasing distance between leg and foothold was monitored by the change in fluorescence resonance energy transfer (FRET) signal. Adapted with permission from Qu *et al.*,^[114] and Tomov *et al.*^[116].

1
2 In addition to DNA nanostructures, there are also nanomaterials in microfluidics that enhance
3
4 the sensing performance of aptamers. The first example of such integration was performed by
5
6 Langer's group in 2005 ^[117]. They conjugated aptamer targeting transmembrane prostate
7
8 specific membrane antigen (PSMA) to PEGylated poly(lactic acid) nanoparticles. The nano-
9
10 conjugate could adhere to cells seeded in microchannel and resist at least 15 times higher shear
11
12 force than the nanoparticle without aptamer. This additional barrier of shear force enhanced the
13
14 specificity of the detection. Since PSMA is a cell surface epitope of prostate cancer, the same
15
16 group also demonstrated the use of this nanoparticle to encapsulate cisplatin and docetaxel for
17
18 target drug delivery.^[118] The nanoparticle was synthesized by nanoprecipitation using a
19
20 microfluidic device that controlled the flow rate of polymers and drug hence the size of
21
22 nanoparticle. Simplifying the design of such microfluidic devices for more practical
23
24 applications at a lower cost is important. In 2012, a three-dimensional microfluidic system was
25
26 built on a paper-folding origami for point of care diagnosis. ^[90] The paper surface was modified
27
28 with porous gold nanoparticle for generation of an electrochemiluminescence signal. The
29
30 incorporation of an ATP aptamer to the nanoparticle led to the detection limit of 0.1 pM. A
31
32 similar concept was applied to another paper microfluidic device (μ PAD) as a colorimetric
33
34 assay to detect cocaine and kanamycin with the limit of detection of 7.78 nM and 3.35 nM
35
36 respectively.^[92a] A platinum nanoparticle functionalized carbon nanotube for the detection of
37
38 mercury ion as an indication of environmental contamination also demonstrated a detection
39
40 limit of 56 pM.^[119]

41
42 Single microfluidic devices allow multiplexed detection for cost-effective diagnosis.^[88a, 120] In
43
44 one study gold nanorods were conjugated to three aptamers; thrombin-binding aptamer,
45
46 immunoglobulin E binding aptamer and PSMA.^[120a] The aptamer modified gold nanorods were
47
48 immobilized into channels on a microfluidic chip then the antigen sample was injected along
49
50 the main channel. Detected target led to a proportional response in localized surface plasmonic
51
52
53
54
55
56
57
58
59
60
61
62
63
64
65

1 resonance that could be detected by dark-field microscopy. Different designs of microfluidic
2 chip were also found to detect multiple foodborne pathogens with colorimetric signal in food
3 samples.^[120b] The detection of *Salmonella enterica*, *Escherichia coli*, and *Listeria*
4 *monocytogenes* reached the limit of detection of 10 colony-forming unit (CFU) per mL. All
5 these studies show the versatility of using DNA nanostructures and microfluidics for both
6 biomedical and bioelectronic applications.
7

8
9 Our group previously developed three DNA nanostructures with different mechanisms for the
10 detection of malaria biomarker *Plasmodium falciparum* lactate dehydrogenase (PfLDH).^[9d-f]
11 First, we were able to use a protein target to open the lid of a DNA origami box through strand
12 displacement.^[9d] We subsequently developed a split aptamer which facilitates a closing
13 mechanism for DNA nanotweezers.^[9e] The presence of PfLDH closed the tweezers and led to
14 the formation of a complete G-quadruplex which catalyzed a peroxidase reaction which
15 generated a diagnostic signal.^[9d, 9e] Large quantities of reagents were required to compare the
16 performance of nanostructures during the optimization process. Microfluidic technology could
17 allow for a more precise optimization process and therefore provide a reduction in the
18 development costs. For diagnostic purposes, we also studied the efficiency of various DNA
19 polyhedra which enhanced the sensitivity of PfLDH aptamer.^[9f] The elevation of the aptamer
20 from the coated surface lowered the dissociation constant six-fold. This enhancement could
21 potentially eliminate false-negative results providing a more reliable diagnosis.^[82a] Together
22 with the integration in microfluidics such as the one made by the Pei group,^[114] we can foresee
23 the development nanoscale biosensors for preventive diagnosis with much higher sensitivity
24 and reliability.
25
26
27
28
29
30
31
32
33
34
35
36
37
38
39
40
41
42
43
44
45
46
47
48
49
50
51

52 **4. Conclusion and Future Perspectives**

53
54 Microfluidic technologies have thoroughly enhanced aptamer-based technologies, from
55 aptamer selections to aptamer-based biosensors. One of the earliest microfluidic methods to
56 benefit aptamer researchers was capillary electrophoresis, a microfluidic method that has been
57
58
59
60
61

1 further improved with droplet microfluidics and has been used to discover an array of important
2 aptamers. Micromagnetic beads have complemented both microfluidics and aptamer research,
3
4 first benefiting researchers looking to partition aptamer bound complexes from solution they
5
6 have been developed into integrated systems that can perform entire rounds of SELEX and has
7
8 resulted in the discovery of a range of important aptamers. IVC is a method which has taken
9
10 SELEX to a new paradigm, in which aptamers are selected not only for binding, but also for
11
12 catalytic activity. Based on droplet microfluidics an array of DNA structures has been
13
14 developed to catalyse a range of chemical reactions. Aptamer based microfluidics have enabled
15
16 improvements in biosensing for whole cells, proteins, and small molecules. This is ultimately
17
18 highlighted by implantable microfluidic devices that can measure the concentration of
19
20 biomarkers in the whole blood of live rats. Despite all the successes, it is clear that we are still
21
22 at an early stage of discovery at the interface between microfluidics and aptamer technology.
23
24
25
26
27
28

29
30 Microfluidic aptamer selection has many possible application and research directions. IVC has
31
32 been utilized for the selection of nucleic acid aptamers to expand selection type from the simple
33
34 binding and single turnover catalysis of classical SELEX, to the more exotic properties such as
35
36 turn on fluorescence upon aptamer/target binding and multiple turnover catalysis. Selections
37
38 can potentially be imagined for any assay that can be linked to a fluorogenic reporter. This
39
40 opens a huge number of potential of research directions including catalysis, bioprocessing and
41
42 photonics.
43
44
45

46
47 Aptamer based microfluidic systems in general, whether they be for selection or sensing, allow
48
49 for increasing throughput, decreasing experimental complexity and increasing sensitivity of the
50
51 assay experiment being performed. These three experimental characteristics are paramount to
52
53 converting labour-intensive, expensive lab based assays into a format that is suitable for
54
55 translational applications. There is likely an important future for aptamer-based microfluidic
56
57
58
59
60
61
62
63
64
65

sensing across disease detection, biosecurity, environmental monitoring and a wide range of other areas.

5. Acknowledgements

This work was supported by Hong Kong University Grants Council under Research Grants Council (RGC) General Research Fund (GRF) grants 17163416 and 17127515 to JAT, and under General Research Fund (GRF) grants 17304514 and 17329516 to HCS.

Received: ((will be filled in by the editorial staff))

Revised: ((will be filled in by the editorial staff))

Published online: ((will be filled in by the editorial staff))

References

- [1] aA. D. Ellington, J. W. Szostak, *Nature* **1990**, *346*, 818; bC. Tuerk, L. Gold, *Science* **1990**, *249*, 505.
- [2] aD. Shangguan, Y. Li, Z. Tang, Z. C. Cao, H. W. Chen, P. Mallikaratchy, K. Sefah, C. J. Yang, W. Tan, *Proceedings of the National Academy of Sciences* **2006**, *103*, 11838; bG. Mayer, *Angewandte Chemie International Edition* **2009**, *48*, 2672-2689; cM. Mascini, I. Palchetti, S. Tombelli, *Angewandte Chemie International Edition* **2012**, *51*, 1316-1332.
- [3] S. D. Jayasena, *Clinical Chemistry* **1999**, *45*, 1628.
- [4] aY. Wan, Y.-t. Kim, N. Li, S. K. Cho, R. Bachoo, A. D. Ellington, S. M. Iqbal, *Cancer Research* **2010**, *70*, 9371; bY. Hathout, E. Brody, P. R. Clemens, L. Cripe, R. K. DeLisle, P. Furlong, H. Gordish-Dressman, L. Hache, E. Henricson, E. P. Hoffman, Y. M. Kobayashi, A. Lorts, J. K. Mah, C. McDonald, B. Mehler, S. Nelson, M. Nikrad, B. Singer, F. Steele, D. Sterling, H. L. Sweeney, S. Williams, L. Gold, *Proceedings of the National Academy of Sciences* **2015**, *112*, 7153; cE. S. Gragoudas, A. P. Adamis, E. T. Cunningham, M. Feinsod, D. R. Guyer, *New England Journal of Medicine* **2004**, *351*, 2805-2816.
- [5] L. H. Lauridsen, R. N. Veedu, *Nucleic Acid Therapeutics* **2012**, *22*, 371-379.
- [6] J. B. H. Tok, N. O. Fischer, *Chemical Communications* **2008**, 1883-1885.
- [7] G. Pothoulakis, F. Ceroni, B. Reeve, T. Ellis, *ACS Synthetic Biology* **2014**, *3*, 182-187.

- [8] aK. D. Warner, M. C. Chen, W. Song, R. L. Strack, A. Thorn, S. R. Jaffrey, A. R. Ferré-D'Amaré, *Nature Structural & Molecular Biology* **2014**, *21*, 658; bN. Svensen, Samie R. Jaffrey, *Cell Chemical Biology* **2016**, *23*, 415-425.
- [9] aS. M. Douglas, I. Bachelet, G. M. Church, *Science* **2012**, *335*, 831; bS. Li, Q. Jiang, S. Liu, Y. Zhang, Y. Tian, C. Song, J. Wang, Y. Zou, G. J. Anderson, J.-Y. Han, Y. Chang, Y. Liu, C. Zhang, L. Chen, G. Zhou, G. Nie, H. Yan, B. Ding, Y. Zhao, *Nature Biotechnology* **2018**, *36*, 258; cQ. Mei, R. H. Johnson, X. Wei, F. Su, Y. Liu, L. Kelbauskas, S. Lindsay, D. R. Meldrum, H. Yan, *Nano Research* **2013**, *6*, 712-719; dM. S. L. Tang, S. C.-C. Shiu, M. Godonoga, Y.-W. Cheung, S. Liang, R. M. Dirkwager, A. B. Kinghorn, L. A. Fraser, J. G. Heddle, J. A. Tanner, *Nanomedicine: Nanotechnology, Biology and Medicine* **2018**, *14*, 1161-1168; eS. C.-C. Shiu, Y.-W. Cheung, R. M. Dirkwager, S. Liang, A. B. Kinghorn, L. A. Fraser, M. S. L. Tang, J. A. Tanner, *Advanced Biosystems* **2017**, *1*, 1600006; fC. S. Shiu, A. L. Fraser, Y. Ding, A. J. Tanner, *Molecules* **2018**, *23*.
- [10] A. I. Taylor, V. B. Pinheiro, M. J. Smola, A. S. Morgunov, S. Peak-Chew, C. Cozens, K. M. Weeks, P. Herdewijn, P. Holliger, *Nature* **2014**, *518*, 427.
- [11] J. W. Jorgenson, K. D. Lukacs, *Analytical Chemistry* **1981**, *53*, 1298-1302.
- [12] X. Lou, J. Qian, Y. Xiao, L. Viel, A. E. Gerdon, E. T. Lagally, P. Atzberger, T. M. Tarasow, A. J. Heeger, H. T. Soh, *Proceedings of the National Academy of Sciences* **2009**, *106*, 2989.
- [13] A. Autour, E. Westhof, M. Ryckelynck, *Nucleic Acids Research* **2016**, *44*, 2491-2500.
- [14] A. L. Fraser, B. A. Kinghorn, S. M. Tang, Y.-W. Cheung, B. Lim, S. Liang, M. R. Dirkwager, A. J. Tanner, *Molecules* **2015**, *20*.
- [15] J. J. Agresti, B. T. Kelly, A. Jäschke, A. D. Griffiths, *Proceedings of the National Academy of Sciences of the United States of America* **2005**, *102*, 16170.
- [16] aL. Huang, S. Bian, Y. Cheng, G. Shi, P. Liu, X. Ye, W. Wang, *Biomicrofluidics* **2017**, *11*, 011501; bM. Selmi, M. H. Gazzah, H. Belmabrouk, *Scientific Reports* **2017**, *7*, 5721; cY.-J. Liu, S.-S. Guo, Z.-L. Zhang, W.-H. Huang, D. Baigl, M. Xie, Y. Chen, D.-W. Pang, *ELECTROPHORESIS* **2007**, *28*, 4713-4722; dJ. P. Brody, P. Yager, *Sensors and Actuators A: Physical* **1997**, *58*, 13-18; eB. S. Ferguson, D. A. Hoggarth, D. Maliniak, K. Ploense, R. J. White, N. Woodward, K. Hsieh, A. J. Bonham, M. Eisenstein, T. E. Kippin, K. W. Plaxco, H. T. Soh, *Science Translational Medicine* **2013**, *5*, 213ra165; fV. Thiviyanathan, D. G. Gorenstein, *PROTEOMICS – Clinical Applications* **2012**, *6*, 563-573.
- [17] aG. M. Whitesides, *Nature* **2006**, *442*, 368; bL. Y. Yeo, H.-C. Chang, P. P. Y. Chan, J. R. Friend, *Small* **2011**, *7*, 12-48.
- [18] T. M. Squires, S. R. Quake, *Reviews of Modern Physics* **2005**, *77*, 977-1026.
- [19] S. K. Sia, G. M. Whitesides, *Electrophoresis* **2003**, *24*, 3563-3576.
- [20] B. H. Weigl, P. Yager, *Science* **1999**, *283*, 346-347.
- [21] C.-Y. Lee, C.-L. Chang, Y.-N. Wang, L.-M. Fu, *International Journal of Molecular Sciences* **2011**, *12*.
- [22] L. Shang, Y. Cheng, Y. Zhao, *Chemical Reviews* **2017**, *117*, 7964-8040.
- [23] J. Nilsson, M. Evander, B. Hammarström, T. Laurell, *Analytica Chimica Acta* **2009**, *649*, 141-157.
- [24] J. Kim, M. Johnson, P. Hill, B. K. Gale, *Integrative Biology* **2009**, *1*, 574-586.
- [25] C.-C. Hong, J.-W. Choi, C. H. Ahn, *Lab on a Chip* **2004**, *4*, 109-113.
- [26] C. Wyatt Shields Iv, C. D. Reyes, G. P. López, *Lab on a Chip* **2015**, *15*, 1230-1249.
- [27] F. Lan, B. Demaree, N. Ahmed, A. R. Abate, *Nature Biotechnology* **2017**, *35*, 640.
- [28] V. Lecault, M. VanInsberghe, S. Sekulovic, D. J. H. F. Knapp, S. Wohrer, W. Bowden, F. Viel, T. McLaughlin, A. Jarandehi, M. Miller, D. Falconnet, A. K. White, D. G.

- Kent, M. R. Copley, F. Taghipour, C. J. Eaves, R. K. Humphries, J. M. Piret, C. L. Hansen, *Nature Methods* **2011**, *8*, 581.
- [29] J. W. Parks, M. A. Olson, J. Kim, D. Ozcelik, H. Cai, R. Carrion, J. L. Patterson, R. A. Mathies, A. R. Hawkins, H. Schmidt, *Biomicrofluidics* **2014**, *8*, 054111.
- [30] G. Luka, A. Ahmadi, H. Najjaran, E. Alocilja, M. DeRosa, K. Wolthers, A. Malki, H. Aziz, A. Althani, M. Hoorfar, *Sensors* **2015**, *15*.
- [31] S. Sakuma, F. J. J. o. R. Arai, *Journal of Robotics and Mechatronics* **2013**, *25*, 277-284.
- [32] S. M. Lunte, D. M. Radzik, in *Progress in Pharmaceutical and Biomedical Analysis, Vol. 2* (Eds.: S. M. Lunte, D. M. Radzik), Elsevier, **1996**, pp. 3-21.
- [33] S. D. Mendonsa, M. T. Bowser, *Journal of the American Chemical Society* **2004**, *126*, 20-21.
- [34] M. Berezovski, A. Drabovich, S. M. Krylova, M. Musheev, V. Okhonin, A. Petrov, S. N. Krylov, *Journal of the American Chemical Society* **2005**, *127*, 3165-3171.
- [35] M. V. Berezovski, M. U. Musheev, A. P. Drabovich, J. V. Jitkova, S. N. Krylov, *Nature Protocols* **2006**, *1*, 1359.
- [36] S. Javaherian, M. U. Musheev, M. Kanoatov, M. V. Berezovski, S. N. Krylov, *Nucleic Acids Research* **2009**, *37*, e62-e62.
- [37] J. Tok, J. Lai, T. Leung, S. F. Y. Li, *ELECTROPHORESIS* **2010**, *31*, 2055-2062.
- [38] aJ. Ashley, K. Ji, S. F. Y. Li, **2012**, *33*, 2783-2789; bS. Lisi, E. Fiore, S. Scarano, E. Pascale, Y. Boehman, F. Ducongé, S. Chierici, M. Minunni, E. Peyrin, C. Ravelet, *Analytica Chimica Acta* **2018**, *1038*, 173-181.
- [39] R. Yufa, S. M. Krylova, C. Bruce, E. A. Bagg, C. J. Schofield, S. N. Krylov, *Analytical Chemistry* **2015**, *87*, 1411-1419.
- [40] J. G. Bruno, *Biochemical and Biophysical Research Communications* **1997**, *234*, 117-120.
- [41] A. S. Sadeghi, M. Mohsenzadeh, K. Abnous, S. M. Taghdisi, M. Ramezani, *Talanta* **2018**, *182*, 193-201.
- [42] J. Qian, X. Lou, Y. Zhang, Y. Xiao, H. T. Soh, *Analytical Chemistry* **2009**, *81*, 5490-5495.
- [43] aM. Cho, Y. Xiao, J. Nie, R. Stewart, A. T. Csordas, S. S. Oh, J. A. Thomson, H. T. Soh, *Proceedings of the National Academy of Sciences* **2010**, *107*, 15373; bS. S. Oh, K. M. Ahmad, M. Cho, S. Kim, Y. Xiao, H. T. Soh, *Analytical Chemistry* **2011**, *83*, 6883-6889.
- [44] Q. Wang, W. Liu, Y. Xing, X. Yang, K. Wang, R. Jiang, P. Wang, Q. Zhao, *Analytical Chemistry* **2014**, *86*, 6572-6579.
- [45] G. Hybarger, J. Bynum, R. F. Williams, J. J. Valdes, J. P. Chambers, *Analytical and Bioanalytical Chemistry* **2006**, *384*, 191-198.
- [46] C.-J. Huang, H.-I. Lin, S.-C. Shiesh, G.-B. Lee, *Biosensors and Bioelectronics* **2010**, *25*, 1761-1766.
- [47] C.-J. Huang, H.-I. Lin, S.-C. Shiesh, G.-B. Lee, *Biosensors and Bioelectronics* **2012**, *35*, 50-55.
- [48] H.-I. Lin, C.-C. Wu, C.-H. Yang, K.-W. Chang, G.-B. Lee, S.-C. Shiesh, *Lab on a Chip* **2015**, *15*, 486-494.
- [49] J. Kim, T. R. Olsen, J. Zhu, J. P. Hilton, K.-A. Yang, R. Pei, M. N. Stojanovic, Q. Lin, *Scientific Reports* **2016**, *6*, 26139.
- [50] S.-L. Hong, Y.-T. Wan, M. Tang, D.-W. Pang, Z.-L. Zhang, *Analytical Chemistry* **2017**, *89*, 6535-6542.
- [51] S.-L. Hong, M.-Q. Xiang, M. Tang, D.-W. Pang, Z.-L. Zhang, *Analytical Chemistry* **2019**, *91*, 3367-3373.
- [52] aJ. J. Agresti, E. Antipov, A. R. Abate, K. Ahn, A. C. Rowat, J.-C. Baret, M. Marquez, A. M. Klibanov, A. D. Griffiths, D. A. Weitz, *Proceedings of the National Academy of*

- Sciences* **2010**, *107*, 4004; bA. Fallah-Araghi, J.-C. Baret, M. Ryckelynck, A. D. Griffiths, *Lab on a Chip* **2012**, *12*, 882-891; cM. Ryckelynck, S. Baudrey, C. Rick, A. Marin, F. Coldren, E. Westhof, A. D. Griffiths, *RNA* **2015**, *21*, 458-469.
- [53] J. S. Paige, K. Y. Wu, S. R. Jaffrey, *Science* **2011**, *333*, 642.
- [54] aR. L. Strack, W. Song, S. R. Jaffrey, *Nature Protocols* **2013**, *9*, 146; bT. A. Rogers, G. E. Andrews, L. Jaeger, W. W. Grabow, *ACS Synthetic Biology* **2015**, *4*, 162-166.
- [55] E. V. Dolgosheina, S. C. Y. Jeng, S. S. S. Panchapakesan, R. Cojocar, P. S. K. Chen, P. D. Wilson, N. Hawkins, P. A. Wiggins, P. J. Unrau, *ACS Chemical Biology* **2014**, *9*, 2412-2420.
- [56] A. Autour, S. C. Y. Jeng, A. D. Cawte, A. Abdolazadeh, A. Galli, S. S. S. Panchapakesan, D. Rueda, M. Ryckelynck, P. J. Unrau, *Nature Communications* **2018**, *9*, 656.
- [57] V. Thivyanathan, D. G. Gorenstein, *Proteomics. Clinical applications* **2012**, *6*, 563-573.
- [58] Y. Song, Z. Zhu, Y. An, W. Zhang, H. Zhang, D. Liu, C. Yu, W. Duan, C. J. Yang, *Analytical Chemistry* **2013**, *85*, 4141-4149.
- [59] G. S. Zamay, O. S. Kolovskaya, T. N. Zamay, Y. E. Glazyrin, A. V. Krat, O. Zubkova, E. Spivak, M. Wehbe, A. Gargaun, D. Muharemagic, M. Komarova, V. Grigorieva, A. Savchenko, A. A. Modestov, M. V. Berezovski, A. S. Zamay, *Molecular Therapy* **2015**, *23*, 1486-1496.
- [60] Z. Libo, T. Chuanhao, X. Li, Z. Zhen, L. Xiaoyan, H. Haixu, C. Si, Z. Wei, H. Mengfei, F. Anna, L. Bing, T. Hsian-Rong, G. Hongjun, L. Yi, F. Xiaohong, *Small* **2016**, *12*, 1072-1081.
- [61] L. M. Millner, M. W. Linder, R. Valdes, *Annals of clinical and laboratory science* **2013**, *43*, 295-304.
- [62] J. Smerage, D. Hayes, *British Journal of Cancer* **2006**, *94*, 8.
- [63] J. A. Phillips, Y. Xu, Z. Xia, Z. H. Fan, W. Tan, *Analytical Chemistry* **2009**, *81*, 1033-1039.
- [64] U. Dharmasiri, S. Balamurugan, A. A. Adams, P. I. Okagbare, A. Obubuafo, S. A. Soper, *ELECTROPHORESIS* **2009**, *30*, 3289-3300.
- [65] W. Sheng, T. Chen, R. Kamath, X. Xiong, W. Tan, Z. H. Fan, *Anal Chem* **2012**, *84*, 4199-4206.
- [66] L. R. Huang, E. C. Cox, R. H. Austin, J. C. Sturm, *Science* **2004**, *304*, 987-990.
- [67] D. Udara, B. Subramanian, A. A. A., O. P. I., O. Annie, S. S. A., *ELECTROPHORESIS* **2009**, *30*, 3289-3300.
- [68] S. J. Reinholt, H. G. Craighead, *Anal Chem* **2018**, *90*, 2601-2608.
- [69] aY. Xu, J. A. Phillips, J. Yan, Q. Li, Z. H. Fan, W. Tan, *Analytical Chemistry* **2009**, *81*, 7436-7442; bW. Sheng, T. Chen, R. Kamath, X. Xiong, W. Tan, Z. H. Fan, *Analytical Chemistry* **2012**, *84*, 4199-4206.
- [70] L. Wang, Q. I. N. Zheng, Q. A. Zhang, H. Xu, J. Tong, C. Zhu, Y. Wan, *Oncology Letters* **2012**, *4*, 935-940.
- [71] Y. Song, Y. Shi, M. Huang, W. Wang, Y. Wang, J. Cheng, Z. Lei, Z. Zhu, C. Yang, *Angewandte Chemie International Edition* **2019**, *58*, 2236-2240.
- [72] J. Teng, F. Yuan, Y. Ye, L. Zheng, L. Yao, F. Xue, W. Chen, B. Li, *Frontiers in microbiology* **2016**, *7*, 1426-1426.
- [73] J. Chung, J. S. Kang, J. S. Jurng, J. H. Jung, B. C. Kim, *Biosensors and Bioelectronics* **2015**, *67*, 303-308.
- [74] Z. Altintas, M. Akgun, G. Kokturk, Y. Uludag, *Biosensors and Bioelectronics* **2018**, *100*, 541-548.

- [75] aD. Proudnikov, A. Mirzabekov, *Nucleic acids research* **1996**, *24*, 4535-4542; bP. R. Langer, A. A. Waldrop, D. C. Ward, *Proceedings of the National Academy of Sciences* **1981**, *78*, 6633-6637; cA. Roget, H. Bazin, R. Teoule, *Nucleic acids research* **1989**, *17*, 7643-7651; dJ. Goodchild, *Bioconjugate Chemistry* **1990**, *1*, 165-187.
- [76] I. German, D. D. Buchanan, R. T. Kennedy, *Analytical Chemistry* **1998**, *70*, 4540-4545.
- [77] aY. Liu, T. Kwa, A. Revzin, *Biomaterials* **2012**, *33*, 7347-7355; bY. Liu, J. Yan, M. C. Howland, T. Kwa, A. Revzin, *Analytical Chemistry* **2011**, *83*, 8286-8292.
- [78] W. Zhang, Z. He, L. Yi, S. Mao, H. Li, J.-M. Lin, *Biosensors and Bioelectronics* **2018**, *102*, 652-660.
- [79] Y.-N. Yang, H.-I. Lin, J.-H. Wang, S.-C. Shiesh, G.-B. Lee, *Biosensors and Bioelectronics* **2009**, *24*, 3091-3096.
- [80] aY.-W. Cheung, R. M. Dirkwager, W.-C. Wong, J. Cardoso, J. D'Arc Neves Costa, J. A. Tanner, *Biochimie* **2018**, *145*, 131-136; bY.-W. Cheung, J. Kwok, A. W. L. Law, R. M. Watt, M. Kotaka, J. A. Tanner, *P Natl Acad Sci USA* **2013**, *110*, 15967-15972.
- [81] R. M. Dirkwager, A. B. Kinghorn, J. S. Richards, J. A. Tanner, *Chemical Communications* **2015**, *51*, 4697-4700.
- [82] aL. A. Fraser, A. B. Kinghorn, R. M. Dirkwager, S. Liang, Y. W. Cheung, B. Lim, S. C. Shiu, M. S. L. Tang, D. Andrew, J. Manitta, J. S. Richards, J. A. Tanner, *Biosensors & bioelectronics* **2018**, *100*, 591-596; bR. M. Dirkwager, S. Liang, J. A. Tanner, *ACS Sensors* **2016**, *1*, 420-426; cG. Figueroa-Miranda, L. Feng, S. C.-C. Shiu, R. M. Dirkwager, Y.-W. Cheung, J. A. Tanner, M. J. Schöning, A. Offenhäusser, D. Mayer, *Sensors and Actuators B: Chemical* **2018**, *255*, 235-243; dL. A. Fraser, A. B. Kinghorn, R. M. Dirkwager, S. Liang, Y.-W. Cheung, B. Lim, S. C.-C. Shiu, M. S. L. Tang, D. Andrew, J. Manitta, J. S. Richards, J. A. Tanner, *Biosensors and Bioelectronics* **2018**, *100*, 591-596.
- [83] X. Lin, Q. Chen, W. Liu, J. Zhang, S. Wang, Z. Lin, J.-M. Lin, *Scientific Reports* **2015**, *5*, 9643.
- [84] aH. Xu, K. Gorgy, C. Gondran, A. Le Goff, N. Spinelli, C. Lopez, E. Defrancq, S. Cosnier, *Biosensors and Bioelectronics* **2013**, *41*, 90-95; bL.-D. Li, H.-T. Zhao, Z.-B. Chen, X.-J. Mu, L. Guo, *Sensors and Actuators B: Chemical* **2011**, *157*, 189-194.
- [85] T. Lim, S. Y. Lee, J. Yang, S. Y. Hwang, Y. Ahn, *BioChip Journal* **2017**, *11*, 109-115.
- [86] S. R. Shin, Y. S. Zhang, D.-J. Kim, A. Manbohi, H. Avci, A. Silvestri, J. Aleman, N. Hu, T. Kilic, W. Keung, M. Righi, P. Assawes, H. A. Alhadrami, R. A. Li, M. R. Dokmeci, A. Khademhosseini, *Analytical Chemistry* **2016**, *88*, 10019-10027.
- [87] aR. W. Hanson, *Biochemical Education* **1989**, *17*, 86-92; bM. Koupenova, K. Ravid, *Journal of cellular physiology* **2013**, 10.1002/jcp.24352.
- [88] aH. Zhang, X. Hu, X. Fu, *Biosensors and Bioelectronics* **2014**, *57*, 22-29; bX. Wei, T. Tian, S. Jia, Z. Zhu, Y. Ma, J. Sun, Z. Lin, C. J. Yang, *Analytical Chemistry* **2016**, *88*, 2345-2352; cY. Zhang, D. Gao, J. Fan, J. Nie, S. Le, W. Zhu, J. Yang, J. Li, *Biosensors and Bioelectronics* **2016**, *78*, 538-546; dH. Fu, J. Yang, L. Guo, J. Nie, Q. Yin, L. Zhang, Y. Zhang, *Biosensors and Bioelectronics* **2017**, *96*, 194-200; eY. Du, C. Chen, M. Zhou, S. Dong, E. Wang, *Analytical Chemistry* **2011**, *83*, 1523-1529.
- [89] Q. Wu, H. Shen, H. Shen, Y. Sun, L. Song, *Talanta* **2016**, *150*, 531-538.
- [90] J. Yan, M. Yan, L. Ge, J. Yu, S. Ge, J. Huang, *Chemical Communications* **2013**, *49*, 1383-1385.
- [91] L. Ge, P. Wang, S. Ge, N. Li, J. Yu, M. Yan, J. Huang, *Analytical Chemistry* **2013**, *85*, 3961-3970.
- [92] aL. Wang, G. Musile, B. R. McCord, *Electrophoresis* **2018**, *39*, 470-475; bJ. P. Hilton, T. H. Nguyen, R. Pei, M. Stojanovic, Q. Lin, *Sensors and Actuators A: Physical* **2011**, *166*, 241-246; cJ. Zhou, A. V. Ellis, H. Kobus, N. H. Voelcker, *Analytica Chimica Acta* **2012**, *719*, 76-81; dJ. S. Swensen, Y. Xiao, B. S. Ferguson, A. A. Lubin, R. Y. Lai, A.

- J. Heeger, K. W. Plaxco, H. T. Soh, *Journal of the American Chemical Society* **2009**, *131*, 4262-4266.
- [93] aY. Ma, Y. Mao, D. Huang, Z. He, J. Yan, T. Tian, Y. Shi, Y. Song, X. Li, Z. Zhu, L. Zhou, C. J. Yang, *Lab on a Chip* **2016**, *16*, 3097-3104; bR. Guider, D. Gandolfi, T. Chalyan, L. Pasquardini, A. Samusenko, C. Pederzoli, G. Pucker, L. Pavesi, *Sensing and Bio-Sensing Research* **2015**, *6*, 99-102.
- [94] P. B. Lillehoj, F. Wei, C.-M. Ho, *Lab on a Chip* **2010**, *10*, 2265-2270.
- [95] aR. Liu, Y. Huang, Y. Ma, S. Jia, M. Gao, J. Li, H. Zhang, D. Xu, M. Wu, Y. Chen, Z. Zhu, C. Yang, *ACS Applied Materials & Interfaces* **2015**, *7*, 6982-6990; bB. Jin, Y. Yang, R. He, Y. I. Park, A. Lee, D. Bai, F. Li, T. J. Lu, F. Xu, M. Lin, *Sensors and Actuators B: Chemical* **2018**, *276*, 48-56; cB. C. Galarreta, M. Tabatabaei, V. Guieu, E. Peyrin, F. Lagugné-Labarthe, *Analytical and Bioanalytical Chemistry* **2013**, *405*, 1613-1621.
- [96] C. Fu, Y. Wang, G. Chen, L. Yang, S. Xu, W. Xu, *Analytical Chemistry* **2015**, *87*, 9555-9558.
- [97] K. Keesung, G. Man-Bock, K. Do-Hyun, P. Jee-Won, S. In-Hong, J. Ho-Sup, S. Kahp-Yang, *ELECTROPHORESIS* **2010**, *31*, 3115-3120.
- [98] C.-C. Wang, J. W. Hennek, A. Ainla, A. A. Kumar, W.-J. Lan, J. Im, B. S. Smith, M. Zhao, G. M. Whitesides, *Analytical Chemistry* **2016**, *88*, 6326-6333.
- [99] I. A. Ges, K. P. M. Currie, F. Baudenbacher, *Biosensors and Bioelectronics* **2012**, *34*, 30-36.
- [100] B. J. Sanghavi, J. A. Moore, J. L. Chávez, J. A. Hagen, N. Kelley-Loughnane, C.-F. Chou, N. S. Swami, *Biosensors and Bioelectronics* **2016**, *78*, 244-252.
- [101] C. Perreard, F. d'Orlye, S. Griveau, B. Liu, F. Bedioui, A. Varenne, *Electrophoresis* **2017**, *38*, 2456-2461.
- [102] aJ. Daprà, L. H. Lauridsen, A. T. Nielsen, N. Rozlosnik, *Biosensors and Bioelectronics* **2013**, *43*, 315-320; bK. Zhang, N. Gan, F. Hu, X. Chen, T. Li, J. Cao, *Microchimica Acta* **2018**, *185*, 181; cD. Desai, M. H. Zaman, *Analytical Methods* **2015**, *7*, 1914-1923.
- [103] P. L. Mage, B. S. Ferguson, D. Maliniak, K. L. Ploense, T. E. Kippin, H. T. Soh, *Nature Biomedical Engineering* **2017**, *1*, 0070.
- [104] S. Zhan, Y. Wu, L. Wang, X. Zhan, P. Zhou, *Biosensors and Bioelectronics* **2016**, *86*, 353-368.
- [105] W. Zhou, R. Saran, J. Liu, *Chemical Reviews* **2017**, *117*, 8272-8325.
- [106] J. A. Phillips, Y. Xu, Z. Xia, Z. H. Fan, W. Tan, *Analytical chemistry* **2008**, *81*, 1033-1039.
- [107] Q. Shen, L. Xu, L. Zhao, D. Wu, Y. Fan, Y. Zhou, W. H. OuYang, X. Xu, Z. Zhang, M. Song, *Advanced Materials* **2013**, *25*, 2368-2373.
- [108] P. Song, D. Ye, X. Zuo, J. Li, J. Wang, H. Liu, M. T. Hwang, J. Chao, S. Su, L. Wang, *Nano letters* **2017**, *17*, 5193-5198.
- [109] T. Tian, X. Wei, S. Jia, R. Zhang, J. Li, Z. Zhu, H. Zhang, Y. Ma, Z. Lin, C. J. Yang, *Biosensors and Bioelectronics* **2016**, *77*, 537-542.
- [110] aN. C. Seeman, *Journal of Theoretical Biology* **1982**, *99*, 237-247; bN. R. Kallenbach, R.-I. Ma, N. C. Seeman, *Nature* **1983**, *305*, 829.
- [111] aP. W. K. Rothmund, *Nature* **2006**, *440*, 297; bB. Wei, M. Dai, P. Yin, *Nature* **2012**, *485*, 623; cL. Qian, Y. Wang, Z. Zhang, J. Zhao, D. Pan, Y. Zhang, Q. Liu, C. Fan, J. Hu, L. He, *Chinese Science Bulletin* **2006**, *51*, 2973-2976.
- [112] aE. S. Andersen, M. Dong, M. M. Nielsen, K. Jahn, R. Subramani, W. Mamdouh, M. M. Golas, B. Sander, H. Stark, C. L. P. Oliveira, J. S. Pedersen, V. Birkedal, F. Besenbacher, K. V. Gothelf, J. Kjems, *Nature* **2009**, *459*, 73; bB. Yurke, A. J. Turberfield, A. P. Mills Jr, F. C. Simmel, J. L. Neumann, *Nature* **2000**, *406*, 605; cR.

- 1 M. Zadegan, M. D. E. Jepsen, L. L. Hildebrandt, V. Birkedal, J. Kjems, *Small* **2015**, *11*,
2 1811-1817; dL. Xin, C. Zhou, Z. Yang, D. Liu, *Small* **2013**, *9*, 3088-3091.
- 3 [113] S. S. Oh, K. Plakos, Y. Xiao, M. Eisenstein, H. T. Soh, *ACS Nano* **2013**, *7*, 9675-9683.
- 4 [114] X. Qu, H. Zhang, H. Chen, A. Aldalbahi, L. Li, Y. Tian, D. A. Weitz, H. Pei, *Analytical*
5 *Chemistry* **2017**, *89*, 3468-3473.
- 6 [115] aJ. Bath, S. J. Green, A. J. Turberfield, **2005**, *44*, 4358-4361; bJ. Mai, I. M. Sokolov, A.
7 Blumen, *Physical Review E* **2001**, *64*, 011102.
- 8 [116] T. E. Tomov, R. Tsukanov, Y. Glick, Y. Berger, M. Liber, D. Avrahami, D. Gerber, E.
9 Nir, *ACS Nano* **2017**, *11*, 4002-4008.
- 10 [117] O. C. Farokhzad, A. Khademhosseini, S. Jon, A. Hermmann, J. Cheng, C. Chin, A.
11 Kiselyuk, B. Teply, G. Eng, R. Langer, *Analytical Chemistry* **2005**, *77*, 5453-5459.
- 12 [118] N. Kolishetti, S. Dhar, P. M. Valencia, L. Q. Lin, R. Karnik, S. J. Lippard, R. Langer,
13 O. C. Farokhzad, *P Natl Acad Sci USA* **2010**, *107*, 17939-17944.
- 14 [119] L. Zhang, Y. Wang, C. Ma, P. Wang, M. Yan, *RSC Advances* **2015**, *5*, 24479-24485.
- 15 [120] aB. Wu, L.-C. Chen, Y. Huang, Y. Zhang, Y. Kang, D.-H. Kim, *Plasmonics* **2014**, *9*,
16 801-807; bX. Wei, W. Zhou, S. T. Sanjay, J. Zhang, Q. Jin, F. Xu, D. C. Dominguez,
17 X. Li, *Analytical Chemistry* **2018**, *90*, 9888-9896.
- 18
19
20
21
22
23
24
25
26
27
28
29
30
31
32
33
34
35
36
37
38
39
40
41
42
43
44
45
46
47
48
49
50
51
52
53
54
55
56
57
58
59
60
61
62
63
64
65



Click here to access/download

Production Data

AdvBioTannerFinal Figures.docx

